AD-A156 602 A REVIEW OF AUSTRALIAN INVESTIGATIONS ON AERONAUTICAL FATIGUE DURING THE..(U) AERONAUTICAL RESEARCH LABS MELBOURNE (AUSTRALIA) G S JOST MAR 85 ARL-STRUC-TM-399 1/3

UNCLASSIFIED F/G 1/3 NL

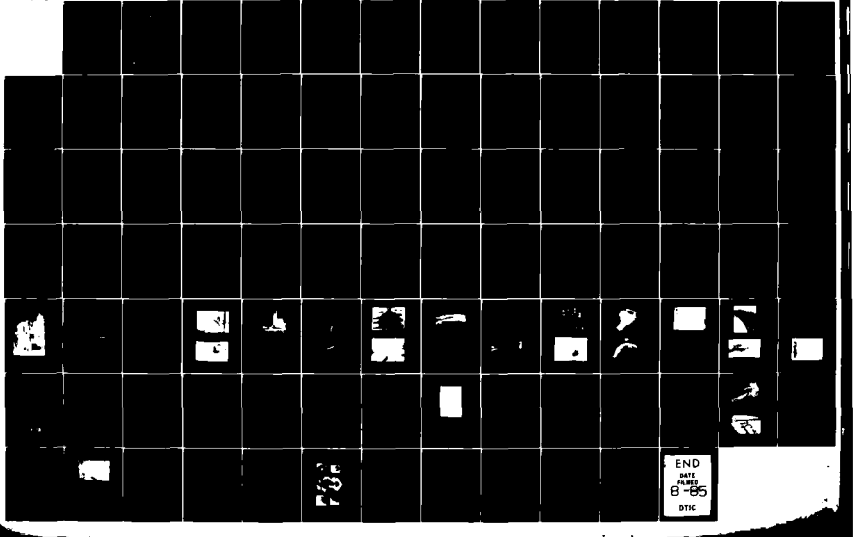

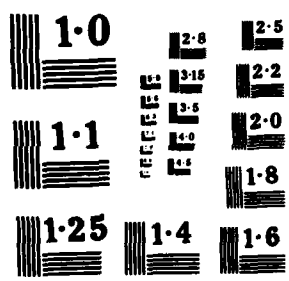
1·0
1·1
1·25
1·4
1·6
1·8
2·0
2·2
2·5
2·8
3·15
3·5
4·0

ARL-STRUC-TM-399

AR-003-993

DEPARTMENT OF DEFENCE

DEFENCE SCIENCE AND TECHNOLOGY ORGANISATION

AERONAUTICAL RESEARCH LABORATORIES

MELBOURNE, VICTORIA

Structures Technical Memorandum 399

A REVIEW OF AUSTRALIAN INVESTIGATIONS ON AERONAUTICAL FATIGUE DURING THE PERIOD APRIL 1983 TO MARCH 1985

Edited by

G.S. JOST

Approved for Public Release

COPY No

MARCH, 1985

AR-003-993

DEPARTMENT OF DEFENCE
DEFENCE SCIENCE AND TECHNOLOGY ORGANISATION
AERONAUTICAL RESEARCH LABORATORIES

Structures Technical Memorandum 399

A REVIEW OF AUSTRALIAN INVESTIGATIONS ON AERONAUTICAL FATIGUE DURING THE PERIOD APRIL 1983 TO MARCH 1985

Edited by

G.S. Jost

SUMMARY

This document was prepared for presentation to the 19th Conference of the International Committee on Aeronautical Fatigue scheduled to be held in Pisa, Italy on May 20 and 21, 1985. It is being distributed within Australia as an ARL Technical Memorandum.

A summary is presented of the aircraft fatigue research and associated activities which form part of the programmes of the Aeronautical Research Laboratories, the Department of Aviation and the Australian aircraft industry. The major topics discussed include the fatigue of both civil and military aircraft stuctures, fatigue damage detection, analysis and repair and fatigue life monitoring and assessment.

POSTAL ADDRESS: Director, Aeronautical Research Laboratories,
P.O. Box 4331, Melbourne, Victoria, 3001, Australia.

CONTENTS

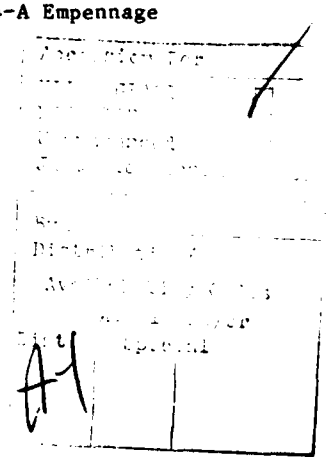

9.1 INTRODUCTION

This Review of Australian investigations on aeronautical fatigue in the 1983 to 1985 biennium has been made possible by the co-operation of the author's colleagues at the Aeronautical Research Laboratories, the Department of Aviation and in the Australian aircraft industry, and their contributions to the Review are gratefully acknowledged. Further information on any item may be obtained from the contacts given. The names, addresses and abbreviations of contributing organisations are as follows:

AAC Australian Aircraft Consortium, Private Bag 14, Port Melbourne, Victoria 3207

ARL Aeronautical Research Laboratories, PO Box 4331, Melbourne, Victoria 3001

CAC Commonwealth Aircraft Corporation Pty Ltd, Box 779H GPO, Melbourne, Victoria 3001

DOA Department of Aviation, PO Box 367, Canberra, ACT 2601

GAF Government Aircraft Factories, PO Box 4, Port Melbourne, Victoria 3207

9.2 FATIGUE OF MILITARY AIRCRAFT STRUCTURES

9.2.1 Mirage IIIO (J.M. Grandage - ARL)

As noted in the previous Australian ICAF Review /1/, cracking detected in service and on the Swiss fatigue test article has led to an assessment being made of the structural integrity of the airframe as a whole. The output of the programme will be inspection schedules for all structural locations which need inspecting to ensure life-of-type. The programme is in some respects similar to the damage tolerance assessments carried out by the USAF on various existing aircraft fleets. Those aspects of the programme which have been in progress in the period 1983-85 include:

a. Selection of structural control points for initial consideration.
b. Development of crack growth modelling techniques.
c. Specimen testing programmes for calibrating and validating crack growth models (see Section 9.4.4).
d. Review of initial material quality to provide a basis for selection of initial flaw sizes.
e. Review of progress on the Swiss fatigue test.
f. Fractographic analyses of cracks produced in the Swiss fatigue test.

g. Flight trials of a strain gauged aircraft aimed at (i) improving knowledge of the strain distribution in fuselage frame 26, and (ii) establishing strain distributions in other components initially considered to be critical.

h. Collection of AFDAS data (Section 9.5.7) which will be used for defining flight load spectra for the fin and rear fuselage.

9.2.2 GAF Nomad (L.T. Tuller - GAF)

The Nomad is an unpressurised, twin turbo-prop aircraft designed and built by the Government Aircraft Factories. It was designed as a utility aircraft with STOL capabilities for operations from short, unprepared airfields. Nomad aircraft are employed in military, civil, geophysical, medical, surveillance and amphibious roles. To date, a total of 170 aircraft have been built.

To aid certification of the aircraft, a full-scale fatigue test of the airframe was undertaken by GAF at ARL. The test began in August, 1976, and is based upon a mean cruise weight of 4180 kg (9200 lb) and a one hour flight profile. Eighty per cent of the total landings are based on operations from prepared airstrips. The flight load spectrum is a severe civil aviation spectrum appropriate to Australian conditions. The ground load spectrum was derived primarily from taxi trial measurements by GAF.

To the beginning of 1985 a total of 165,843 simulated flights have been achieved. The fatigue test was temporarily halted in December, 1982 due to a critical failure of the stub wing front spar upper cap, Fig. 9.1. After an 18 month down-time, the Nomad fatigue test programme was resumed in May, 1984. The original stub-wing assembly was completely removed and replaced by a new test specimen at 137,986 test hours. The new stub-wing structure incorporates some potentially fatigue sensitive parts from the previous test specimen (rear spar, strut pick-up fittings, etc) and a new front spar.

The test continues to reveal some unexpected failures. For example, a major crack was identified in the main wing rib at STA.114, Fig. 9.2. The rib will shortly be replaced. A critical crack has also developed in the front spar upper cap of the new stub wing. The crack location is identical to the previous failure location, but the times to crack initiation differ by a factor of five, Fig. 9.3. This failure could have significant implication for the service life of Nomad aircraft. However, it is envisaged that

regular in-service inspection of the critical areas of the structure, and fractographic results will provide sufficient justification for fatigue life extension.

Failures in the upper cap and web of the original stub wing front spar were investigated by residual strength tests. The objectives of these tests were to correlate fracture mechanics and residual strength test results, and to derive the maximum permissible crack size. These objectives were satisfactorily accomplished for the spar cap only /2/.
The stub wing spar cap residual strength test was followed by fractographic investigation of the fracture face. Figures 9.1 and 9.4 show the starboard failure location, and the fractographically derived crack propagation data. The fracture surface was badly damaged during the test, and the crack propagation data include some gaps. These uncertainties may be resolved by a fractographic examination to be made of the port side spar crack, and the crack in the same location in the second stub-wing.

Although the total number of identified cracks to date is 163 /3/, and most of these cracks are of relatively minor significance, some major or critical cracks have also occurred. A brief summary of the major cracks and failures is provided in Table 9.1. The fatigue test is also providing an ideal opportunity to develop and evaluate possible repair schemes and inspection techniques. For example, a redesigned lower wing skin has survived 54,000 flights without any cracking, whereas the first crack in the original skin was already noted at 4,500 flight hours /4/.

It is envisaged that the Nomad fatigue test programme will continue to beyond 200,000 flight hours. The currently outstanding test objectives include the establishment of fatigue critical areas for the main wing spars, and the stub wing rear spar (a function of ground loading). These objectives are particularly important because the currently known failure locations are not likely to define the economic life of the airframe. Analysis of the main wing spar strain gauges indicate that the magnitude of the test loadings will have to be considerably increased to achieve the above objectives there. The main disadvantage of a revised test load spectrum is the possibility of stub wing front spar failures, and the associated costs and delays.

Several aspects of the Nomad fatigue life certification programme have been revived, and some of these tasks are in progress. Future plans include a new

flight test programme, fatigue testing of part of the wing flight control system, a re-analysis of the taxi trial results and selective monitoring of the real flight spectrum. Strain gauges are being fitted to over one hundred stations in the flight test aircraft to provide results for the verification of the fatigue test loading. These investigations should provide further data for understanding the relationship between the fatigue test results and the service life of the structure.

Some parts of the Nomad airframe are not being fatigue tested (in particular the fin and tailplane) and fatigue certification is being achieved by theoretical analysis only. During 1983/84, recommendations were provided for the replacement of the fin attachment fittings /5/.

9.2.3 CT4-A Air Trainer (C.K. Rider, R.G. Parker - ARL)

The CT4-A Air Trainer is a two-place piston engined fully aerobatic trainer aircraft of 1070 kg all-up weight in service with the Royal Australian Air Force. Since the last report /1/ a full-scale fatigue test has been conducted on a CT4-A Air Trainer airframe. The test began in June 1983 and continued until final collapse was achieved in May 1984. The test article consisted of the basic fuselage structure including engine frame, full mainplane, horizontal tailplane and fin. The main undercarriage legs were also included. Strains were recorded at 70 locations throughout the structure, 16 of which were monitored continuously.

The test rig with the test article in place is shown in Fig. 9.5. The rig and its control systems incorporated several innovative features including:

a. a patented scheme whereby positive and negative loading on the wings is applied via one jack. It overcomes the interaction effects of dual jacks and eliminates crossover distortion in wing strain during excursion through zero load. On the present test article only one jack per wing was required, but the same principle may be applied to larger tests where several jacks may be needed.
b. an active roll compensation system in which wing tip displacement differences and phase are fed back into the main wing load control channels.
c. automatic valve balancing where null balances are performed during startup and at the end of every flight.
d. a computer controlled startup sequence of 16 separate steps to permit the necessary calibrations, safety checks and correct sequencing of hydraulic

valves to be performed safely. The shutdown procedure was also computer controlled to allow load to be shed uniformly. An algorithm to identify structural failure was also incorporated into the shutdown procedure to modify the actions required upon failure.

A sequence of actuator loads defined by fatigue meter records was developed to represent average training squadron usage. These loads represented manoeuvre, gust and ground cycle loading. Trials representing both student and instructor flying were flown by four pilots in six missions covering full fuel and half fuel load conditions. Flight manoeuvre test loads were derived from these 24 flights. Gust loads were derived from flight data modified to match the gust spectrum developed by Sherman /6/ and given in Table 9.2. Ground cycle loads were developed from take-off, touch-and-go, and taxiing load data recorded for bitumen and grass surfaces.

Five load spectra were used in the course of the test, truncated in each case at +6g and -2.5g, the 6g load being applied once per 144 test programmes. A programme contained the complete set of load applications or "turning points" incorporated in a spectrum and represented a number of flights each of which was approximately equivalent to a one hour flight. The preliminary spectrum consisted of 24 flights of 2733 turning points per programme, 36 of which were applied representing 1414 service hours. This spectrum did not include gust, rare loads or heavy undercarriage loads. Rare loads were incorporated in the second spectrum which consisted of 76 flights of 6519 turning points per programme. This spectrum was adjusted after two programmes to increase some loads in the gust flights incorporated within the spectrum thus producing the third spectrum which was applied for 89 programmes.

The fourth and major spectrum was produced when representative undercarriage loads became available - the wing loads remained unchanged. The 76 flights per programme were retained but the number of turning points was changed to 6248. This spectrum was applied for 516 programmes which with the other spectra represented 25,463 simulated service hours as required by the test specification.

Following this test milestone the rate of fatigue damage accumulation was increased by applying a more severe loading spectrum. This fifth spectrum retained the same range but was reduced to 25 flights and increased to 171

hours per programme. This spectrum was applied until port wing failure occurred at 51,141 hours.

The test highlighted four main fatigue prone areas. All were in the mainplane assembly shown in Fig. 9.6. The 5000 hour major inspection revealed considerable fatigue damage in the port wing forward attachment area. It was found by fractographic analysis that the two lowest bolts of the attachment bracket failed at approximately 2500 hours. There was also fatigue cracking in the inter-rib diaphragms and corner stiffening brackets as depicted in Fig. 9.7. The corresponding area in the starboard wing was free of damage and did not fail in this manner until 17,000 hours whereas the port side required frequent bolt replacement throughout the test.

Skin cracking also appeared at 5000 hours in the starboard wing between ribs 5 and 6 on the compression surface as a result of skin buckling. These cracks were repaired by a RAAF standard insert patch as shown in Fig. 9.8. Similar cracking occurred at 6000 hours in the port wing in which repairs were made by a bonded boron fibre patch. These two repair schemes were monitored throughout the test, the boron fibre repair technique giving the best performance.

In the early stages of the test, wing centre section spar cap rivets in the vicinity of the wing root ribs began failing in fatigue. These were replaced by HI-LOK pin fasteners in accordance with Royal New Zealand Air Force practice and no further failures were experienced.

Final failure occurred at 51,141 simulated hours in the port wing main spar tension boom assembly between ribs 1 and 2 as shown in Fig. 9.9. A photograph of the failed boom is shown in Fig. 9.10. and a diagram showing the crack initiation sites and the crack growth in the boom assembly is shown in Fig. 9.11.

9.2.4 Wamira - New RAAF Basic Trainer (G.E. Lawrence - AAC)

The Wamira is an Australian designed, two-place turbo-prop basic pilot training aircraft to be built for the Royal Australian Air Force. It is to replace the present fleet of CT4-A aircraft. Both side-by-side and tandem variants are under development.

The design requirements for the Wamira were identified in the 1983 ICAF Review /1/. The structural design is to satisfy the durability and damage tolerance requirements of MIL-STD-1530A. Damage tolerance principles and analysis techniques have been employed to optimise the design of critical components whilst maintaining minimum weight.

Constant amplitude coupon testing to generate crack growth rate data has been completed for the materials being used in the manufacture of critical components of the Wamira. A comprehensive spectrum loading coupon test programme involving 200 specimens has begun. This programme will evaluate five materials, five flight-by-flight spectra representing critical areas of the Wamira and various levels of through stress and bearing stress. Fractographic examination of the specimen failure surfaces will provide calibration parameters for the computerised crack growth model. The calibrated crack growth model will then be used to establish design stress levels for the aircraft structure.

Component tests of the wing front spar to fuselage lower attachment fitting and tailplane main spar to fuselage attachment fitting are scheduled to begin in March 1985.

The Wamira full-scale durability test is in the detailed planning stages with testing due to start in 1986. It is anticipated that approximately twenty-seven loading jacks will be used to apply representative manoeuvre and landing loads to a complete trainer airframe. The flight-by-flight loading spectrum to be used on the test is based on RAAF specified Nz and landing sinkspeed exceedance requirements. Anticipated aircraft usage during pilot training will be used to establish load and flight sequencing.

9.3 FATIGUE IN CIVIL AIRCRAFT (R.B. Douglas - DOA)

9.3.1 Partenavia P68 Series Aircraft

The Partenavia P68B Victor is a medium weight twin engine high wing monoplane, a number of which are used primarily in remote country operations within Australia. These types of operations, often including high utilization from unprepared runways, are considered to be one possible reason for fuselage frame cracking which was recently found in a P68B aircraft. The cracking occurred in the two main fuselage frames which distribute the concentrated loads from the wing and the landing gear into the fuselage structure.

The cracks were found in frame 8 and frame 9 at the landing gear girder truss attachment bracket locations shown in Fig. 9.12. The starboard side of frame 8 had cracks between the outer attachment bracket holes, running from the lower bolt hole to the frame radius in a downward and outward direction. The crack continued along the radius for approximately 25 mm. Similar cracking was observed on the port side of frame 8, but in this case the crack stopped at the frame radius. Cracking in frame 9 was similar but less severe.

For the last 1800 hours the aircraft had operated from dirt strips, averaging 3 flights per hour. After 1700 hours of this operation the elastomeric cushions between the main landing gear leg and the girder were found missing. This was rectified and the aircraft accumulated a further 100 hours prior to detection of the frame cracks. It has been suggested that inadequate damping of undercarriage ground loads could have been a contributory cause. The frequent dirt strip operations would have accelerated the onset of fatigue cracking.

The manufacturer has responded to the fuselage frame cracking by designing a repair scheme which involves the installation of a doubler over the subject area. This allows most of the undercarriage loads to be distributed away from the cracked frame area and should alleviate any further problem.

While carrying out repairs to the wing of an accident-damaged Partenavia P68 aircraft, cracks were discovered in both front and rear spars. In each case the cracks were located in the horizontal flange of the lower cap angles, at the inboard end where the horizontal flange tapers in width to enable it to pass through the wing-fuselage attachment. Fig. 9.13 shows the four front spar sections as removed from the aircraft.

Subsequent laboratory analysis /7/ revealed that the cracks were caused by fatigue, the contributing factors being:

a. the abrupt change in section,
b. the sharp run-out radius at the end of the taper, and
c. the poor surface finish.

This is illustrated in Fig. 9.14.

The aircraft had completed 3356 hours time in service and an unknown number of flights, whereas the manufacturer's fatigue life analysis had predicted a safe life of 11,800 hours. Striation counting on one fracture surface showed that

the crack had been propagating for at least 1200 flights. Fig 9.15 shows a photo-mosaic of part of the fracture surface.

A fleet inspection was carried out and similar cracks were found in 25% of the aircraft in Australia. Some of these affected aircraft had flown as little as 2000 hours.

Details of the problem were passed to the manufacturer, who has since advised that quality control procedures have been revised and that design changes are in hand to reduce the stress concentration at the critical location in future production aircraft. Inspection procedures and repair kits have been made available for aircraft in service.

One puzzling aspect of this problem, in view of the proportion of the Australian fleet affected, is that there have been no reports of similar cracks found in aircraft operating in other countries.

9.3.2 Cessna Model 210 Tailplane Cracking

The Australian Department of Aviation has received a number of Defect Reports concerning cracked Cessna Model 210 tailplane left hand rear spar reinforcement brackets, Fig. 9.16. All the brackets were cracked in the same location, along the bottom radius from left to right, and in the fore/aft direction through the left hand countersunk screw hole, Fig. 9.17. In one case both the rear spar and doubler reinforcement making up the spar assembly were found cracked at the flange bend radius immediately under the cracked reinforcement bracket. Another recent defect report indicated that the doubler only was cracked.

Two of the cracked reinforcement brackets were subjected to fractographic examination to determine modes of failure. The fracture surfaces showed multiple crack origins, corrosion and fretting which is indicative of low load amplitude, high cycle fatigue. One of the fracture surfaces is reproduced in Fig. 9.18.

The manufacturer conducted an inflight and ground handling strain survey in an attempt to determine the loading condition(s) causing the cracking. In general, the stress levels were consistently higher on the left-hand bracket, with higher stresses showing up in the cruise range. Another possible reason

for the cracking is the vibratory loads induced on the tailplane by the slipstream during engine run-up prior to take-off.

The defect history for the bracket has led to a redesign, and a welded steel bracket now replaces the original aluminium component. To ensure the continued airworthiness of aluminium brackets still in service, the manufacturer has conducted a failsafe analysis to evaluate the effect of the failure modes shown in Fig. 9.18. The area concerned is readily accessible for a visual inspection.

9.3.3 Piper Aerostar 600 - Main Landing Gear Failures

Numerous reports have been received of failures in the main landing gear scissors link in Piper 600 series Aerostar aircraft. Two cracked, and one failed sample are illustrated in Fig. 9.19. Frequent repetitive dye penetrant inspections of these parts have now been made mandatory.

Laboratory analysis /8/ has shown that cracks initiate in the fillet radii adjacent to the single lug. They then propagate by fatigue for a short period until the link encounters a significant manoeuvreing or braking load which causes it to fail, usually during the landing roll. Hence most of the fracture surface is indicative of overload as shown in Fig. 9.20.

The primary problem appears to be one of inadequate static strength, as shown by the relative proportions of the fatigue and overload zones. This explains why failures have also occurred in the "improved" link, which is the same as the earlier link except for an enlarged fillet radius.

It is the Department's view that failures will continue to occur until either the lug thickness is increased, or the link is made from a stronger material.

9.3.4 Propeller Fatigue

During the period under review, propeller fatigue failures in General Aviation aircraft have continued to occur as they have in past years, and have almost come to be accepted as a statistical fact of life. The more "routine" failures are those involving non-catastrophic loss of a blade tip from a rapidly propagating fatigue crack initiating at a stone chip. Occasionally there is a failure, fortunately rare, involving loss of a complete blade with subsequent catastrophic results.

One such failure which occurred recently was a hub failure in a McCauley model D3A 32C90-LM 3-bladed propeller fitted to a Cessna U206F aircraft, Fig. 9.21. The propeller had been in operation for 4987 hours since new, 1363 hours since overhaul and 30 hours since its last 100-hourly periodic inspection. The failure initiated in a known fatigue critical location, in the root of the internal thread which holds the blade retention nut. The fracture surface is shown in Fig. 9.22.

Laboratory examination /9/ showed that the root of the sixth thread, where the crack initiated, had a number of surface notches which appeared to be the result of inadequate shot peening over a localised area, Fig. 9.23. The shot peening coverage of the remainder of the hub was satisfactory and no other material anomalies were observed.

The crack propagation rate was assessed using striation counting and assuming that the major striations represented flight cycles. This work suggested that the crack would have been detectable on the outside surface of the hub at the last 100 hour inspection. It is possible that the presence of a self adhesive decal fixed to the hub in the region of the failure, Fig. 9.21, may have hindered detection of the crack.

Eddy current inspection of the remaining two blade sockets showed that one of these also contained a crack indication in a similar location at the root of the sixth thread. The crack was opened and examined and was also confirmed as fatigue.

9.3.5 Helicopter Fatigue

During the past biennium, two unrelated helicopter fatigue defects occurred which demonstrate the need for strict adherence to manufacturers' maintenance and overhaul instructions.

The first of these involved a fatigue crack which was found in the skin of a Bell 206B main rotor blade. The root end of the blade is reinforced by a number of overlying bonded finger doublers, Fig. 9.24. Should disbonds occur under the end of a doubler, the standard repair scheme is to trim up to 50 mm from the end of the doubler. However, the repair is rather delicate in that great care is required to prevent inadvertent tool damage to the underlying skin. This point is emphasised strongly in the manufacturer's repair and overhaul instructions, and also in operational safety notices.

Laboratory examination /10/ of the cracked blade clearly showed that the crack had originated in an area where the skin had been damaged during such a repair operation. The crack occurred some 433 hours time in service after the repair, at a blade total time of 5620 hours. Fig. 9.25 shows a close-up view of the crack, while Fig. 9.26 shows the fracture surface and the reduced skin thickness. In this instance the crack was found and the blade removed from service before the crack progressed into the blade spar; however, there have been instances overseas where catastrophic blade failure in flight has occurred from this cause.

The second case involved the in-flight failure of an eye bolt end in a Hiller UH-12E helicopter. The shank of the bolt is the attachment point for the main rotor blade tension/torsion strap, whilst the eye end which failed is the attachment for the inboard end of the drag link. It failed after about 600 hours time in service, and it is worth noting that the mandatory fatigue retirement life is 640 hours. Laboratory examination /11/ showed a fatigue failure initiating from multiple origins at corrosion pits in the bore of the eye end. The presence of the corrosion, fretting and wear which can be seen in Figs 9.27 and 9.28, and the absence of any traces of red dye, indicated that the prescribed maintenance which included periodic (150-hourly) lubrication and dye penetrant inspection, had not been carried out.

As with many other failures in the past, these two occurrences once again show that complacency, or non-observance of correct procedures, can lead to unanticipated fatigue failures and that economy-motivated short cuts can have expensive consequences - particularly with helicopters.

9.3.6 Bell Model 212 Lift Link Fitting Cracking

A defect report was recently received from an Australian offshore charter operator concerning failure of a lift link lower attachment fitting lug on a Bell Model 212 helicopter. The lift link transfers the main rotor lift loads into a fuselage bulkhead, Fig. 9.29. This is the first reported occurrence of such a failure in Australia, although there have been reports of cracking of the lift link upper attachment fitting itself.

The defect was discovered during a pre-flight inspection. The fact that the lug was found completely failed is causing some concern at this stage. It appears that the corner cracking which occurred in this defect was not amenable to visual inspection prior to final failure.

The fitting is currently being subjected to a complete fractographic analysis. Preliminary results from the examination of wear patterns on the inside surface of the lugs indicate a possible lift link misalignment problem. The subsequent fretting between the flange of the steel bush insert and the hole of the lug is a possible cause of crack initiation, since at this stage no evidence of any manufacturing defects or corrosion has been discovered near the crack origin. The fracture surface shows a regular pattern of striations possibly indicative of the major flight cycle, Fig. 9.30. Finer striation markings are also evident between the major markings. An inspection of the lead time Australian Bell 212 did not reveal any similar cracking. The investigation is still in progress.

9.3.7 Fatigue of Fibre Reinforced Plastic Gliders

In the 1983 review /1/ mention was made of a proposal to carry out a full scale fatigue test on a 'Janus' glass fibre reinforced wing. This project is proceeding, albeit slowly. The test specimen comprises one brand new wing, which has an extensive array of strain gauges installed during manufacture, and one wing which was repaired after severe accident damage, to try and assess the long-term effect of major repairs to FRP structures.

Much has been done since the proposal was first initiated, but there have been delays. Design of the test rig could not be finalised until the load distribution could be established with confidence, but the rig has now been designed and construction begun. The load controller and hydraulic equipment have also been procured.

Flight testing is proceeding and flight loads, load distribution and strain data have been accrued in training, pleasure and competitive flying. The test is scheduled to begin running by June 1985.

9.4 FATIGUE DAMAGED STRUCTURE: DETECTION, ANALYSIS AND REPAIR

9.4.1 Mirage Fatigue Life Extension Programme (J.Y. Mann - ARL)

In the 1981 and 1983 Australian ICAF Reviews details were given of an extensive investigation on small specimens representing the rear and front flanges of the main spar of the Mirage III wing. This testing programme was carried out to develop refurbishment techniques which would allow the fatigue life of that particular part of the structure to be extended to meet a new life-of-type requirement. The results of this investigation have been published in a number of ARL reports /12-16/ and other publications /17,18/.

Fractographic investigations on the thick (32 mm) specimens provided a considerable amount of information relating to variability in fatigue crack initiation and propagation /15/. A good linear relationship was found between the log. life and log. crack depth for individual specimens, Fig. 9.31. At the smallest crack depth used for analysis (0.3 mm) no significant differences were found between the standard deviations of log. life to crack initiation, for crack propagation or to final failure, nor in the corresponding standard deviations of arithmetic lives. However, in considering the more general question of whether the greater contribution to variability in total life comes from that in initiation life or that in propagation life, it was shown that cognizance must be taken of the analytical basis of the assessment - whether arithmetic or logarithmic, Fig. 9.32. On an arithmetic basis the standard deviation of life to the formation of the crack increases with increasing crack depth, whereas on a logarithmic basis it decreases. The converse applies in each case for the variability in propagation lives. On an arithmetic basis the standard deviation of the crack propagation rate increases with crack depth, Fig. 9.33(b), that at a depth of 5 mm being about seven times that at a crack depth of 0.5 mm. On the other hand, the standard deviation of log. crack propagation rate is substantially constant irrespective of crack depth.

Refurbishment of the main spar by the insertion of interference-fit steel bushes was adopted for 89 wings in the RAAF Mirage III fleet. However, some wings could not be refurbished by this method because fatigue cracks at the bolt holes were larger than the limits which had been defined, and the edge distance of an adjacent rivet hole was less than the minimum specified for satisfactory refurbishment. During the past two years supplementary investigations have been carried out to explore methods for providing a further increase in life of the main spar. These have included specific tests relating to the rivet holes, and tests involving a redesigned section at the critical part of the spar.

(i) Rivet holes. Fatigue tests were carried out on simple single-hole and twin-hole specimens in which the holes were treated in a number of ways including cold-expansion and the installation of adhesively-bonded rivets. Although cold-expansion provided a 40% increase in life compared to open reamed holes, the fatigue lives of specimens with adhesively-bonded rivets were about 2.5 times those with open holes /19/. A finite-element analysis showed that adhesive-bonding significantly reduces both the local stress

concentration at the hole and stress intensities at the crack tips, thus retarding crack initiation and reducing crack propagation rates. Fractographic investigations confirmed that the crack propagation rates in adhesively-bonded rivet specimens were only about half those in specimens with open holes, Fig. 9.34.

Additional tests on large rear flange specimens identical to those used previously but incorporating adhesively-bonded rivets in the single leg anchor nut (SLAN) rivet holes did not indicate such an increase in life. Although the increase was useful it was only about 30% more than that of specimens with open SLAN rivet holes. Tests were also carried out on large rear flange specimens which incorporated interference-fit steel pins in the SLAN rivet holes. These indicated fatigue lives more than double those of specimens with open SLAN rivet holes.

(ii) Redesigned Mirage spars. The redesign involved an increase in section thickness and an increase in width of the flange (which allowed an increase in the edge distance of the bolt holes), together with the elimination of all rivet holes in the critical area of the flange. Two groups of specimens were tested, namely those in which the bolt holes were cold-expanded using the Boeing process, and those in which interference-fit bushes were fitted in the bolt holes. The log. average fatigue lives of the relevant groups of specimens were as follows:

Original design of spar:	6200 flights
Original design, bolt holes bushed, SLAN rivet holes empty:	9200 flights
Original design, bolt holes bushed, SLAN holes bonded rivets:	12100 flights
Original design, bolt holes bushed, SLAN holes interference pins:	15100 flights
Redesign, cold-expanded bolt holes:	53300 flights
Redesign, interference-bushed bolt holes:	43100 flights.

The difference between the last two conditions probably reflects the change in nett-section resulting from the incorporation of an 11 mm outside diameter bush at the first bolt hole instead of an 8 mm diameter bolt.

9.4.2 Fatigue Life Enhancement Fastener Programme (J.Y. Mann, G.S. Jost, R. Jones - ARL)

Fastener holes are a primary source of fatigue cracking in aircraft structures. Increasing demands to extend the service lives of structures past those originally designed for, and the continuing quest for minimum structural weight to improve aircraft performance, have resulted in the development of specific fatigue-life-ehancement systems for holes in structural joints /20/. Most of these systems are based on the premise that a reduction in the severity of the localised fatigue loadings will increase life.

A general review /21/ has been made of the stress fields associated with holes containing interference-fit fasteners and holes cold-expanded to provide beneficial residual stress fields. This revealed significant shortcomings in some models used to predict residual stress fields and little experimental evidence to verify predicted stress fields. Similarly, little appears to be known of residual stresses around holes in thick sections. The review has provided the base for several studies begun in the past biennium aimed at resolving some of the above uncertainties.

The case of an elastic interference-fit disc near the free edge of a semi-infinite plate has been studied analytically using the concept of a pressurized hole /22/. For the same geometry, the exact elastic solutions for stress and displacement for a bonded interference-fit disc of the same material have been evaluated /23/, Fig. 9.35, and compared with the earlier solution /24/. The conditions leading to the initiation of yielding with and without remote loading have also been determined /25/. Finite element predictions of stress and strain for a large plate containing two closely spaced interference-fitted holes have been compared with experimental data /26/.

Finite element analysis is also being used in a numerical study simulating the cold-expansion process. In the first phase, a hole in a large plate having the characteristics of an aluminium alloy is being expanded incrementally up to 5% of diameter. Incremental unloading will follow. Subsequently, the influences of neat-fit and interference-fit pins together with pin and remote loading combinations are to be investigated.

In another investigation, a penalty element method for the stress analysis of interference-fit pin and cold-expanded holes has been developed /27/. The method is applicable to both two- and three-dimensional problems, and was used to examine stress and displacement fields through the thickness of a finite thickness plate. A full three-dimensional, elastic-plastic, finite element analysis was carried out for a hole expansion of 0.5% in a circular aluminium alloy plate 40 mm in diameter, 12.5 mm thick containing an 8 mm diameter hole. Because of axisymmetry, only a small sector required examination. The free-surface displacement profile shown in Fig. 9.36 suggests that, for thick plates, three-dimensional analysis may well be necessary for the accurate estimation of stress and strain fields in practice.

Recent experimental work has shown that adhesively-bonded inserts can significantly increase the fatigue life of fastener holes. In /28/ attention is focussed on developing an understanding of the mechanism responsible for the observed increase in life. It is shown that the stress concentration factor at an uncracked hole and the stress intensity factor for a cracked hole are significantly reduced if the hole contains a bonded rivet, Fig. 9.37, or a steel sleeve. Further, as crack length increases, the solution for a single-cracked hole containing a bonded insert of the same material approaches that for the crack alone, ie. with no hole in the specimen.

The next stage in this project will comprise a three-dimensional numerical and experimental investigation into the repair of a quadrant crack emanating from a fastener hole.

9.4.3 Experimental Stress Measurement (J.G. Sparrow - ARL)

The Aeronautical Research Laboratories have recently taken delivery of a SPATE 8000 Thermoelastic stress analyser. This instrument, developed and marketed by Ometron Ltd in the UK, provides a measurement of alternating stress fields (sum of principal stresses) for its monitoring of the cyclic temperature changes. These temperature changes are calculated from the measured 10 - 14 micron infrared emission band, and SPATE is therefore able to achieve a resolution down to a dimension of about 0.5 mm and sensitivity of the order of 400 kPa (60 psi) for aluminium. The load frequency range of operation is 0.5 Hz to 20 kHz.

The SPATE 8000 instrument makes possible a degree of speed and versatility for the measurement of cyclic stresses not otherwise available. It is proposed

to deploy the instrument on a number of projects including studies of methods of fatigue life enhancement of bolt holes, stress mapping of complex geometries, intercomparison with finite element analyses and crack initiation investigations. Measurements on both metallic and composite material specimens are planned.

Work is continuing on research into the use of ultrasonic shear wave birefringence as a means of measuring residual stresses. The programme is currently concerned with an evaluation of three proposed methods for separating the effects of stress and texture on the ultrasonic velocity.

Instrumentation is being developed for the automatic recording of in-plane Moire fringe patterns using a technique based on digital recording of a solid state camera output. Software for automatic analysis into strain contours is being written. Initially this method will be applied to the measurement of strain fields around cold-expanded bolt holes. Photoelastic coatings applied to both entry and exit sides of a specimen prior to cold working of the hole with the split sleeve method allows comparison of the two stress fields. This has shown an asymmetry in the stress field adjacent to the split in the sleeve, particularly on the side from which the cold working mandrel entered, Fig. 9.38.

The standard blind hole drilling method of measuring residual stresses is applicable only to strain fields uniform with depth /29/. A study has begun to assess whether the method can be extended to enable quantitative determination of shallow stress fields which vary with depth. Measurements using an ultra high speed drill will be compared with predictions from a finite element analysis.

9.4.4 Fatigue Crack Growth Prediction (J.M. Finney - ARL)

To assure the safe operation of Australia's Mirage aircraft is has been necessary to make predictions of crack growth in fuselage frame 26 which contains the main attachments for the delta wings. For this purpose constant- and variable-amplitude fatigue crack growth data have been obtained for A7-U4SG-T651 (2214) aluminium alloy enabling calibration of computer models for predicting crack growth in frame 26 /30/. The constant-amplitude data were obtained at three R-values using centre-cracked-tension (CCT) specimens of 5 mm and 20 mm thickness. The 20 mm-thick specimen data are shown in Fig. 9.39; the 5 mm-thick specimen results were similar.

The variable-amplitude tests were made on both CCT specimens and specimens simulating two regions of frame 26 of the Mirage fuselage. The simulation specimen configurations are given in Figs 9.40 and 9.41. The sequence was derived from that used by the Swiss Federal Aircraft Factory (F+W) at Emmen, for testing Mirage III aircraft. Additional variable-amplitude tests were made using a RAAF 'all-time-average' sequence for Mirage aircraft.

The crack growth prediction program CRACKS IV was used with the constant- and F+W variable-amplitude crack growth data from CCT specimens to calibrate various crack growth models. In particular, the four retardation models contained in CRACKS IV were examined - Wheeler, Willenborg, modified Willenborg and Crack Closure. Calibration of the Wheeler exponent, m, was achieved by comparing the experimental crack growth curve, using CCT specimens, with the curves predicted using various m-values, as shown in Fig. 9.42. The results for the 20 mm thick specimens were:

Stress (MPa)/g	m-value
17.98	1.50
13.33	0.75

As found by others, /31/, the Wheeler exponent is stress level dependent, but the dependence can be accounted for with a number of calibration tests, Fig. 9.43. A similar stress level dependence of the modified Willenborg shut-off ratio, S, was found, the results in this case being:

Stress (MPa)/g	S-value
17.98	2.2
13.33	3.0

No attempt was made to calibrate the six parameters of the Crack Closure model /32/ and published values for 2024-T3 were used.

Crack growth in the frame-bottom simulation specimen was predicted for the F+W sequence using a Wheeler exponent of 4.2 obtained from the calibration above, and good agreement was obtained with the experimental result. Prediction of the hole-18 test result using Wheeler however revealed a discrepancy by a factor of about eight. Crack growth was predicted for the CCT specimen tested under the RAAF 'all-time-average' sequence using the four retardation models and the results are shown in Fig. 9.44. Reasonable predictions are made by the Wheeler and modified Willenborg models only. These two models

were then used to predict crack growth in a frame-bottom simulation specimen and a very poor result was obtained, Fig. 9.45.

The following conclusions can be drawn from these results:

1. Of the four retardation models considered, the Wheeler and modified Willenborg models are the most satisfactory.
2. When the loading sequence and specimen geometry are different from those used in calibrating the retardation models, none of the models yield accurate predictions.
3. Crack growth life in aircraft structures may not be confidently predicted to better than a factor of two on actual life and, in some cases, the factor may be as high as ten.

9.4.5 Crack Closure and the Growth of Defects in Fatigue (J.Q. Clayton - ARL)

A theoretical study, using the Dugdale Model, has been initiated to investigate crack closure at small defects /33/. At such defects the crack closure process is complicated because the particular form of contact is not constant, as in steady-state fatigue, but changes as the defect grows. As a consequence, the crack-opening load (or stress intensity) is found to increase with crack length until the steady-state condition is reached. This crack length would appear to represent the point beyond which conventional linear elastic fracture mechanics analysis can be reliably applied.

A related study, again employing the Dugdale Model, is being undertaken to investigate the role of material thickness in fatigue. Since this model normally provides, at best, a two-dimensional model of the fatigue process, a further variable, representing the constraint developed in a particular material thickness, has been introduced. This approach is being used in an attempt to describe the retardation due to overloads in aluminium alloy test pieces of differing thicknesses.

9.4.6 Analysis and NDI of a Failed Helicopter Drive Pinion (N.T. Goldsmith - ARL)

Following the failure of the power input pinion (a spiral bevel gear) from a Westland Wessex helicopter in service, which resulted in the loss of the aircraft, an investigation into the growth of the critical fatigue crack was undertaken. This was done to provide an initial estimate of a safe inspection interval, and to develop a crack growth model to predict the growth

of the fatigue crack from the initiating defect under a realistic load spectrum.

The fatigue crack in the gear, Fig. 9.46, initiated from a surface-breaking inclusion in the tooth root, then grew along the length of the root while slowly increasing in depth, finally penetrating the wall of the hollow gear. The crack then grew around the base of the gear, where the gear boss attached to the gear shaft, eventually separating when some three quarters of the base was cracked. The gear boss was then thrown from the gearbox by the crown wheel, smashing through the casing and the flight control mechanisms, resulting in loss of pilot control and loss of the aircraft.

As a precaution following this service failure, new pinions were installed in each gearbox throughout the fleet. Each new pinion was inspected prior to installation, as were those removed from service, using fluorescent magnetic particle inspection designed to concentrate on the critical tooth root area. In addition, a subsequent microscopic examination was made of any suspect location. Only one defective pinion was found during this inspection programme, and that has been returned to the manufacturer for independent assessment.

The first estimate of the crack growth rate was based on the spacing of crack propagation markings, Fig. 9.47, where they were still visible, on the undamaged parts of the fracture surface. Experience with fatigue cracks has shown that, in general, so long as the crack shape remains geometrically similar, then a plot of log crack depth or area versus cycles is essentially linear. Taking this behaviour as a working hypothesis, it then becomes possible to construct a crack growth curve, plotting data points were they are available, and "filling in the gaps" by joining each discontinuity with smooth joining lines, the desired result being a "smooth curve". When the crack changes shape however, usually because of the changing geometry of the component through which the crack is growing, the slope of the crack growth curve is also likely to change. By careful consideration of the changes of the crack shape in the gear, together with the results from the measurement of the progression markings, a crack growth curve was produced which covered the latter stages of the life of the crack, Fig. 9.48. The early part of the crack growth showed no progesssion markings or fatigue striations, the surfaces having been well polished by the working together of the crack faces.

These gearboxes are being monitored in service with a vibration analysis technique, and recordings make of the failed gearbox (before failure) were afterwards subjected to analysis directed at picking out any unusual features in the power spectrum of the power input pinion. The results indicate that a crack may have been detectable by this means some 30 hours before failure and may have just possibly have been detectable some 100 hours before failure - these findings are wholly consistent with the fractographic analysis.

The second part of the investigation is current, and requires adequate data for the purpose of successfully modelling the crack growth in the complex stress field in the gear. The sources of this complexity are:

1. The residual stress distribution produced by the carburised case of the gear and its heat treatment condition.
2. Any modification of this stress distribution produced by the final machining of the gear.
3. The stress distribution superimposed upon the residual stress by the applied load, a combination of shear and bending, complicated by the sliding friction loads developed in spiral bevel gears.
4. The interaction of the initiating defect geometry with the stresses present to produce a stress-intensity factor.
5. The interaction of the crack geometry with the stress field to produce a crack having the observed shape.
6. Obtaining data for crack growth in the bevel gear material, in the various conditions, ie. through the case to the core.
7. Obtaining data for the rapid tearing growth which occurred during the latter part of the crack development.
8. Assembling all of these factors into a model which successfully predicts the crack shape and growth rate, where this is known.

The parameters which affect the shape of the crack as it develops from the initiating defect have been explored, and found to depend strongly upon the stress distribution through the depth of the gear wall in the tooth root. The work is continuing using a finite element model of the stress distribution in the tooth root which will, it is hoped, produce a more accurate representation of the stress distribution.

9.4.7 Load Cycle Reconstitution (J.M. Finney - ARL)

Crack growth accelerations and retardations are significant and widely-researched phenomena and they lead to an expectation that the method of

reconstituting a load sequence will have a substantial effect on crack growth life. An experimental program is well advanced to determine the range of crack growth lives that may be obtained by reconstitution. There is no doubt that quite arbitrary sequences, eg. a single overload in an otherwise constant-amplitude pattern, can give rise to a large range of lives depending on the methods of counting and reconstituting cycles and the relative program length. The experiments below, however, have explored reconstitution of a flight-by-flight fighter sequence and used specimens representative of a wing spar. The flight-by-flight sequence, comprising 500 flights and 109,000 turning points, was that used in a full-scale test of a Mirage wing. The sequence was counted using the range-pair technique and all reconstitutions yielded the same range-pair table, Table 9.3.

Four reconstitutions were developed, two promoting crack growth acceleration (denoted A1, A2) and two promoting retardation (R1, R2). A1 followed the simple acceleration principle - precede the largest loads with the smallest loads. This was achieved by following successive diagonals of the range-pair table, each of constant load range but decreasing mean load, commencing with the highest peak and tough. The simple retardation sequence, R1, was the reverse of A1. The second acceleration sequence, A2, was a development of A1 and utilized additional features:

i. randomise or continuously fluctuate successive load levels.
ii. follow immediately the largest positive peaks with a negative trough.
iii. gradually reduce successive peaks following the largest peaks.

Items ii. and iii. above reduce crack growth retardation.

Sequence R2 made use of the following features for retarding crack growth:

i. follow the largest peak in the sequence with all peaks expected to give no subsequent crack growth, ie. utilise the phenomenon of crack arrest.
ii. after the application of a large peak load, take account of the phenomenon of delayed retardation in order to minimize subsequent growth rates.
iii. apply multiple rather than single large-peak loads to enhance the amount of retardation.

A minimum of five specimens simulating an area of the rear flange of the Mirage wing main spar, were tested under the original flight-by-flight sequence and the four reconstituted sequences noted above. Average lives are listed in Table 9.4; there is no significant difference between the means or

the variances of log. total life of the five sequences examined. Fractographic analysis is proceeding to establish whether this conclusion applies also to crack growth life.

Centre-cracked-tension specimens have been tested under sequences A2 and R2 to ascertain whether the lack of sequence effect obtained with the simulation specimens is dependent on either geometry or stress level. The results are presented in Fig. 9.49 and average best-fit curves are indicated for both sequences. At a stress level of 11.0 MPa/g covering lives up to about 40 programmes (20,000 flights), there is no significant difference between the average crack growth curves. At 17.0 MPa/g, covering lives up to about 10 programmes (5000 flights), retardation sequence R2 gives significantly faster crack growth than acceleration sequence A2. The difference however is small - less than 15%.

The general conclusion from this study that fatigue life (and crack growth life in particular) is little affected by the details of reconstitution is encouraging and a fortunate one for aircraft fatigue load recorders, most of which delete time information. It is also important in crack growth prediction. A final series of tests to establish whether random reconstitutions give the same crack growth behaviour as the extreme reconstitutions used above is underway.

9.4.8 Composites in Aircraft Structures (B.C. Hoskin, R. Jones - ARL)

9.4.8.1 Box beam investigation

Preparations are well underway for a fatigue test on a 2.5 m long box-beam specimen comprising a 56-ply XAS/914 graphite/epoxy skin (28 plies at 0°, 28 plies at $\pm 45^{\circ}$) attached by titanium fasteners to an aluminium alloy sub-structure, Fig. 9.50. The main aim of the test is to examine the growth of barely visible impact damage that will be inserted in the composite skin prior to test. The specimen was manufactured for ARL by British Aerospace, Warton, UK. The load spectrum will be derived from FALSTAFF Mission 2 by removal of a substantial number of low loads. Initially, the test will be conducted in the ambient environment but later it is intended to include the effects of moisture absorption and temperature excursions, representative, as far as is possible, of supersonic fighter usage.

9.4.8.2 Damage tolerance of composites

Tests and analyses performed at ARL and RAE Farnborough /34,35/ have led to a new hypothesis concerning impact damage of composites viz:

> "A stage is reached after which any further significant increase in impact damage does not result in a significant decrease in residual strength".

The analytical tools developed to predict failure are based on fracture mechanics principles and rely heavily on the finite element method. An advanced super-element has been specifically developed for this problem /36/ and a detailed review of the effects of delamination damage can be found in /37/.

9.4.8.3 Repair of thick sections

A detailed design study has been completed into the repair of surface flaws in thick aluminium alloy components (typically of the order of 12mm) using boron epoxy patches /38/. The analysis predicts substantial increases in fatigue life. This has been confirmed by a series of laboratory tests undertaken on 11 mm thick x 108 mm wide x 300 mm long 2024-T4 specimens containing a 37 mm long surface crack 6 mm deep. The unpatched specimens sustained on average approximately 25,000 cycles at 5 $\pm$ 5 ksi whilst the patched specimen survived more than 700,000 cycles at the same stress level and more than 11,000 cycles at 10 $\pm$ 10 ksi.

9.4.9 Crack Patching Technology (A.A. Baker - ARL)

Several developments have been made with crack patching technology, as described in Australian ICAF reviews since 1977. The repair procedure /39/ involves the use of unidirectional boron/epoxy composite patches which are adhesively bonded over the cracked region, thereby reducing stress-intensity and slowing down or preventing further crack growth. Aspects described below are (i) development of improved patch application procedures, and (ii) evaluation of patching design allowables.

9.4.9.1 Development of minimum patch application procedures and processes

Ideally, for several reasons including ease of field application, the adhesives used for crack patching should cure at relatively low temperatures and pressures and provide a high level of bond strength and durability following a simple surface treatment of the bonding surface. Since previous

studies had established the superiority of epoxy-nitrile type film adhesives for patching - particularly for high stress applications, further work was undertaken to establish (i) minimum cure temperatures and times, and (ii) minimum surface-treatments.

minimum adhesive cure temperatures /40/

Studies were made to assess the minimum temperature at which useful cure of the adhesive AF126 could be achieved and, in addition, some tests were also performed on adhesive FM73. Both adhesives are nitrile-rubber modified epoxies for which the recommended cure time is 1 hr at 120°C under a pressure of 0.3 MPa. FM73 is a state-of-the-art adhesive with improved storage life under refrigeration and increased working life at ambient temperature compared to AF126. In part, the improvement results from the increased resistance of FM73 to hydrolysis in the presence of atmospheric moisture.

The level of cure was assessed using infrared spectroscopy to follow the progress of the cure reaction. Spectra were run at intervals on a sample mounted in the spectrometer in an assembly. The disappearance of the epoxy band ($915cm^{-1}$) is taken as an indication of apparent cure. The results of this experiment lead to the minimum effective cure times listed in Table 9.5. The rate of reaction of FM73 differs from AF126 because the two systems contain different curing agents.

Finally, tension tests were performed on single overlap specimens made with these adhesives. The results for tests performed at 20°C or 80°C, listed in Table 9.6, show that for cure times consistent with Table 9.5 only a small penalty appears to be incurred by use of the low cure temperatures. It is of interest to note the fairly poor result at elevated temperature for the 8h/80°C cure of AF126 where 25-30% of the epoxide groups should have been unreacted.

minimum surface-treatment and adhesive cure conditions /41/

Studies were aimed at evaluating (a) the influence of reduced cure temperature on bond durability, and (b) use of silane to improve bond durability and to simplify surface-treatment procedures.

Silanes are extensively employed as coupling agents (or primers) to improve the durability of bonds between adhesives and inorganics such as glass or

metals. Briefly, the silane molecule, on hydration in water, can be represented by the following simplified formula

$$R \text{ ---------- } S_1(OH)_3$$

The $S_1(OH)_3$ group is thought to react with the surface of the inorganic to form a strong covalent bond leaving the organofunctional group, represented by R, free to react with the adhesive during its subsequent cure; thus R must be a group which is chemically compatible with the particular adhesive employed. The silane used to promote bonding of epoxy adhesives to aluminium is usually γ-glycidoxypropyl-trimethoxysilane (γ-GPS) in which R is an epoxy grouping which is compatible with epoxy adhesives. In the present study Union Carbide silane A-187 (γ- APS) was evaluated on clad 2024-T3 prepared either by phosphoric acid gel anodising or by grit-blasting. Adhesives AF126 or FM73 were used to form Boeing wedge-test specimens and were cured at 80°C, 100°C or the standard 120°C, under either mechanical pressure or vacuum bag conditions. The results on these specimens are provided in Table 9.7. Low crack growth in the adhesive during the wedge test is the main indication of high bond durability.

The results for AF126 show that, for surface-treatment by the phosphoric acid gel anodising procedure, durability is good with the 100°C and 120°C cure but shows a significant reduction at 80°C. As noted previously, durability is very poor when grit-blasting alone is employed for the surface-treatment. Use of the silane primer, however, appears to be highly beneficial, particularly with the specimens surface-treated by grit-blasting. FM73, compared to AF126, appears to provide a reduced level of durability with phosphoric acid gel anodise, particularly at the lower cure temperatures. However, the improvement gained by using the silane primer with either surface-treatment is quite dramatic.

From these results it appears that adhesives FM73, and possibly AF126, will provide excellent durability with an 80°C cure following surface treatment of the metallic adherends by grit-blasting and a silane primer.

9.4.9.2 Evaluation of patching design allowables /42/

The three basic requirements to avoid patch failure in crack-patching are that (a) the strain capability of the reinforcement should not be exceeded, (b) the shear stress or strain capability of the adhesive system (for adhesive or

cohesive failure - whichever is the lowest) should not be exceeded, and (c) the length of the patch must be sufficient to allow development of a full elastic trough in the adhesive layer. Aspects (a) and (b) are presently under investigation, the aim being to obtain allowable values, in the case of the adhesive, for representative environmental and temperature conditions. Some studies on the adhesive are briefly described here.

Studies at ambient conditions have been performed on the elemental joint specimen, Figs 9.51(a) and (b). The main measurement is of opening Δ versus cycles N at constant tension/zero cycling to peak load intensity - load per unit width (2F). Allowing for the strain in the reinforcement over length h, the displacement δ (directly related to the shear strain γ in the adhesive, through $\gamma = \delta/2t$) can be determined from Δ. Figure 9.52 shows the results of δ versus N for a boron/epoxy reinforced specimen tested at two levels of (2F). At the relatively low loading frequency used, considerable creep δ_c occurs, and permanent damage occurs, as indicated by the divergence of the curves for δ_c and δ_T. Although the divergence between the curves could be explained as cracking of average length a* in the adhesive, optical microscopy revealed no gross cracking. Thus, it is conjectured that the damage may take the form of crazing or more subtle deterioration of the polymer structure - further studies employing electron microscopy are in progress to clarify this aspect.

If the apparent crack size a* is plotted against N, Fig. 9.53, straight line relationships result. This behaviour is consistent with the constant G predicted for disbond growth in this joint configuration. It is also noted that similar specimens with aluminium outer adherends appear to be much more resistant to damage in the adhesive layer - probably due to the absence of residual stresses in this case.

From the preliminary data obtained to date, it is tentatively concluded that for the AF126 adhesive system a value of 0.2 be taken for the allowable peak shear strain under ambient conditions to avoid excessive fatigue damage.

9.4.9.3 Stress analysis of double overlap fatigue specimen /43/

A finite element analysis of the elemental joint specimen shown in Figs 9.51 (also called the double overlap fatigue specimen, DOFS) has revealed that the approximate one-dimensional theory used in the past is inaccurate in the

vicinity of the crack (ie. the gap in the specimen) and that a two-dimensional analysis of the joint configuration is required.

A particularly significant finding is that fibre and adhesive stresses are strongly dependent on gap size: in the specimen the gap size should therefore be as small as possible to simulate accurately a patched crack.

9.5 FATIGUE LOADS, LIFE MONITORING AND ASSESSMENT

9.5.1 Atmospheric Turbulence and a New Innovation to the Aircraft Meteorological Data Relay (AMDAR) System (D.J. Sherman - ARL)

AMDAR is a system of measuring wind speed, wind direction, air temperature and an indicator of turbulence from INS equipped aircraft in flight. These data are transmitted by radio to the meteorological data system.

The prototype AMDAR system was developed during the mid 1970's and used primarily the ASDAR transmission system to relay the data at hourly intervals through meteorological satellites. A later variant, which is presently being implemented in Australia, uses the ACARS relay through the ARINC or the SITA/AIRCOM networks to relay the data at much more frequent intervals.

The early AMDAR system did not report any indication of turbulence. After some years of experience with the prototype system /44/ it has become apparent that certain additional features are desirable. One of these is the ability to report turbulence in addition to wind velocity. The basic indicator of turbulence is the vertical acceleration of the aircraft measured at (or near) the centre of gravity, and an early proposal was to report a turbulence parameter generated from accelerometer data and formatted according to a slight modification of the ICAO (1970) recommendations for PIREPS. In this proposal turbulence was simply divided into four categories depending on the aircraft vertical acceleration:

MEASURED PEAK ACCELERATION DEVIATION	TURBULENCE CATEGORY
0g - 0.2g	Nil
0.2g - 0.5g	Light
0.5g - 1.0g	Heavy
Over 1.0g	Severe

It is recognised, however, that this categorisation was chosen for PIREPS because of limitations on the time and amount of information available to a pilot making a report. A computerised data acquisition system is capable of reporting a much more sophisticated index of turbulence.

One of the problems of using aircraft accleration alone as a measure of turbulence is that a given gust in the atmosphere will cause different accelerations to different aircraft. To a first order of approximation, the vertical acceleration of an aircraft varies directly with airspeed and inversely with weight. A simple measure of the severity of the actual atmospheric gust strength can be calculated from the parameters available on the aircraft's integrated data system. This measure is the "derived equivalent gust velocity", which is to be used in the new Australian implementation /45/.

When turbulence is reported in terms of derived equivalent gust velocity it is possible to use the data to prepare a climatology of turbulence. (Each report is archived and includes the latitude, longitude and altitude at the time of transmission - a sample of the proposed output format is shown in Fig. 9.54). The AMDAR/ACARS system is being fitted to Boeing 767 aircraft of a local airline, Ansett Airlines of Australia.

The derived equivalent gust velocity is computed from the formula

$$U_{de} = A(m/V_c)\,\Delta n$$

where m is the aircraft mass in metric tonnes, V_c is the calibrated air speed in knots, Δn is the increment in the aircraft acceleration, measured in units of g, and U_{de} is reported in tenths of m/s. For a typical height/mach number profile A is a function of height H(kft) and aircraft mass m given by

$$A = 18 + [300/(30 + H)][(3/8 + 5/8 \times 100/m)]$$

Severe turbulence corresponds to derived equivalent gust velocities in excess of 9 m/s.

9.5.2 Safe Operation of Cracked Structure (J.M. Grandage - ARL)

Existing airworthiness requirements for military aircraft are directed towards the designer rather than the fleet operator, and do not appear to cover the

case of continued operation of aircraft which have cracks in primary structure. While the need to assess existing fleets against the new USAF design requirements has been recognised, no formal requirements or guide-lines appear to have been issued for such applications.

In /46/ a procedure is developed for operating a fleet on a safety-by-inspection basis, given that an in-service inspection programme has shown cracks to exist in primary structure of some aircraft, and that aircraft are permitted to continue operating if their cracks were seen to be below a defined size at the most recent inspection. The aim of the procedure is to ensure that, given this situation, the risk of catastrophic failure is maintained consistent with values implied by the existing design requirements. It is assumed that operation with known cracks is justified by the improvements in NDI sensitivity which enable cracks to be detected at such

a small size that the residual strength is not significantly impaired, even allowing for continuing crack growth during the following inspection interval.

The procedure is formulated for two cases: first, when all the fleet has been inspected at least once, and will continue to be inspected periodically at the structural location(s) under discussion. The procedure then obtains estimated inspection intervals and rejection criteria which should ensure reasonable safety levels. The second case is when only a proportion of the fleet has been inspected and some aircraft are found to be cracked. In this case an additional output is the estimated time to the first inspection for the remainder of the fleet.

The paper summarises the design requirements, emphasising their problems in the present context and illustrating these problems with some case studies. This leads to a statement of the procedure and a discussion to its application.

9.5.3 Rainflow Counts in Random Noise (D.G. Ford - ARL)

One of the basic theoretical problems in fatigue prediction is the distribution of damaging loads, essentially countable, over continuous time. For example exceedances/hour relate to this question.

It is clear that initiation, and to some extent crack growth, depend on the distribution and frequency of range-mean pairs. The counting of these in

observed load histories is well developed, /47,48/, but until now there has been little corresponding theory.

Under conditions which guarantee finite occurrence rates, the average frequency of a specified range pair exceedance in stationary Gaussian random noise defined by its autocorrelation function (hence its power spectrum) has now been derived. The exceedance is defined in terms of two conditional upcrossings and the work extends that of others on simpler processes. For practical purposes it requires computer implementation and this is to be provided for the outputs of linear systems.

9.5.4 Risk and Reliability (D.G. Ford - ARL)

Apart from slow Monte Carlo simulations, the ARL NERF program remains the only single-crack package for fatigue life and inspection analysis which allows for variability in crack growth rate, initiation time and residual strength. Since the publication of /49/, two further reports /50, 51/ have been produced as programming and user manuals, and further development is proceeding.

At the Waloddi Weibull Memorial Symposium sponsored by IUTAM in Stockholm in June 1984, four Australian authored papers were presented, one of which /52/ used the NERF program. Hasofer's paper /53/ dealt with an extension of the Weibull distribution and Leicester presented some exact solutions for realistic structural risk problems /54/.

The fourth paper /55/ described a general framework for fatigue with several interacting failures in which the life distribution follows from given damage and crack growth laws. The damage laws provide boundary conditions for a transport equation description of crack size density. If the diffusion term in the transport equation is neglected, the density of crack sizes is governed by a continuity equation for probability with boundary conditions supplied by damages equivalent to initiation probabilities. For all structures, the set of such damages may be thought to occupy a hypercube in damage space. This multi-crack model is now being programmed as a simulation model with critical damages uniformly distributed in the damage cube.

9.5.5 Resonance Fatigue Testing of the CT4-A Empennage (I.A. Anderson - ARL)

In the flight tests flown to establish strain data for the full-scale fatigue test on the CT4-A Air Trainer (Section 9.2.3), it had been observed that unexpectedly high empennage strains occurred under some conditions. As these

proved to be associated with resonance rather than manoeuvre loadings, a resonance fatigue test of this part of the structure was carried out.

An appropriate block programme sequence of loads from 30 to 100% of maximum load was applied at the resonant frequency of nine Hertz, Fig. 9.55. Numerous failures were detected from 3-1/2 hours of testing time through to cessation of the test at 16 hours, Fig. 9.56. This time corresponds to many tens of thousands of normal flight hours, and neither the empennage nor the associated fuselage structure is expected to cause difficulty during the life-of-type of the aircraft.

9.5.6 NDI Research (I.G. Scott - ARL)

Progress in nondestructiv inspection (NDI) research has continued along the lines described in the previous review.

Acoustic emmission (AE) monitoring of a full-scale fatigue test on a fighter aircraft has continued, but along different lines from those originally intended. It had been proposed to seek directly a relationship between crack growth and selected AE parameters. However, crack growth information available from NDI and fractography has been unsatisfactory, and different approaches have been necessary. So far tests have been conducted on two different wings.

The testing equipment /56/ has performed reasonably well although amendments have been necessary from time-to-time. In addition, some changes have been made as a result of data analysis /57/. AE data was collected in two different ways - on cassette tape and on 9-track computer tape. The cassette tape data comprised records of load, pulse height and rise time of all AE events and some necessary data for identification. This was taken continuously when the AE equipment was operating. The tape data comprised waveforms of AE events and was obtained on command. Analysis of the cassette data was evaluated in terms of difference between data from flaw-free and cracked holes and in terms of the position in the load cycle where signals occurred. No strong relationship was found. The waveform data were analysed in terms of spectral parameters /58/ and this work is continuing.

The test article is complex and the test situation is very noisy (for AE measurements); in addition, the changes in test method, due to the absence of crack growth data, have meant that use of a non-ideal approach has been

necessary. However the project has provided an excellent opportunity to undertake AE measurements on practical structure.

Further studies on source identification have been undertaken - it has been confirmed that, at least in one aircraft aluminium alloy, the dominant source of AE is the cracking of inclusions under fatigue test conditions /59/, and some interesting overload effects have been identified /60/. A preliminary study of accuracies and location of AE sources has been undertaken /61/. In another investigation /62/ to quantify the relationship between acoustic emission (AE) and fatigue crack growth in 4340 steels, it was found that AE can, under some conditions, be quite erratic. If used as an indicator of fatigue crack growth in such steels, AE may, therefore, be quite misleading, and give rise to potentially dangerous situations.

Work has begun on basic studies of the eddy current test technique, on theoretical studies of wave propagation in plates and on the further development of computer-controlled NDI equipment.

9.5.7 Fatigue Monitoring of RAAF Aircraft (R.C. Beckett - CAC)

9.5.7.1 F-111C aircraft monitoring

The monitoring of F-111 aircraft of the RAAF has been characterised by individual aircraft tracking using counting accelerometer data, component modification and movements information to allow the assignment of life data to serial number components, and the collection of flight parameter records from a sample of the fleet. A relatively high return rate of counting accelerometer data has been achieved, but a relatively low rate of flight parameter records on the more complex recorder has been achieved. Nevertheless the flight recorder data have been put to good use in some special investigations. It was found that maintaining a good quality component data tracking base is not a straight-forward operation and the lessons learned have been applied to monitoring arrangements for other aircraft. Some 26 areas of the airframe and landing gear are being monitored, and comprehensive reports are being produced every six months. Two areas of the aircraft have been highlighted as potentially critical by fatigue monitoring and special investigations have been undertaken for these areas.

The recorded information has been used to good advantage to help resolve a problem in the wing upper plate which led to premature cracking of the

aircraft. It has been possible to trace the individual aircraft history and to correlate that with fractographic information from fatigue fractures taken from aircraft which failed in a cold proof load test /1/. As part of the Australian programme to react to this problem, the flight parameter recorder was modified to record some strains. This yielded useful information about limit load conditions and loads which it was suspected may have caused some fatigue damage that would otherwise not have been conveniently studied.

In the future, the RAAF intends to monitor each individual F-111 using AFDAS* equipment. Currently, a prototype AFDAS equipped aircraft is being fitted with strain gauge sensors at 16 separate locations. This aircraft is due to fly in March 1985.

9.5.7.2 Mirage aircraft monitoring

All Mirage aircraft of the RAAF fleet are fitted with fatigue meters. In addition, ten of these have now been fitted with AFDAS equipment. Vertical acceleration, wing strain, wing support structure strain and fin support structure strain transducers are fitted to each aircraft. The reliability of the equipment has been quite high, the greatest problem in acquiring data having been in interrogating the on-board unit. Nevertheless, a good return of data has been obtained and has provided the basis for studies of the effect of placard limits and the comparison of strain spectra at various locations around the aeroplane with fatigue test strain spectra.

A data base for assessing the effect of different kinds of future flying on crack growth or fatigue damage has proved to be a valuable fatigue management tool.

CAC has provided engineering support to a Mirage Durability and Damage Tolerance Assessment Programme. This involved the review of all the accelerometer data for the complete previous history of all aircraft by tail number and the forecasting of strain spectra for individual aircraft using these data and the AFDAS records obtained on the fleet sample. Crack growth and fatigue damage models have been developed which use AFDAS data directly as

* For a description of the Australian designed and built Aircraft Fatigue Data Analysis System (AFDAS) see /63/.

input. This has involved great economies of computing, and provided a sound basis for individual aircraft tracking using a DADTA approach. Calculations are based on a flight by flight crack growth model rather than a load by load model. A number of CAC reports describing this work have been produced in the period.

9.5.7.3 F/A-18 fatigue monitoring

CAC is well advanced in the development of a computer based system for life monitoring on the engine and airframe of the F/A-18 entering service with the RAAF in 1985. Each aircraft has been fitted with a flight parameter and strain recorder by the manufacturer, McDonnell Douglas, but RAAF aircraft will also have a 12 channel, second generation, AFDAS device fitted. This enables broader coverage of the airframe, and AFDAS is configured to pick up much higher frequency vibrations than the maintenance data recorder system. The Mk III AFDAS unit also automatically reads and stores individual flight data. The total system will consist of a dedicated computer and various flight recorder interface equipment for each operating squadron, along with a central computer at CAC to analyse the longer term life information. Data will be used by operating squadrons to help in fault finding of service aircraft.

9.5.7.4 Macchi MB326H fatigue life monitoring

A detailed specification for an enhanced computer based fatigue life monitoring system for Macchi aircraft has been developed. One aircraft has been fitted with an AFDAS recording system as a prototype, and when this installation has been proven, a sample of the aircraft in the fleet will be fitted with AFDAS units. Selected gauge locations are on the wing, wing carry-through structure, vertical tail, and horizontal tail support structure.

9.5.7.5 Nomad aircraft life monitoring

Specifications for a computer based system for monitoring fatigue life consumption on the Nomad have been developed. A modification proposal for fitting AFDAS equipment to a small sample of the fleet has also been developed.

9.5.7.6 Wamira service usage loads history forecast

In support of design activities on the new Australian designed basic training aircraft, Wamira (Section 9.2.4), CAC has developed techniques for determining loads histories from expected usage spectra. The technique involves a

hierachial structure where the aircraft usage is defined in terms of loads associated with various flight environment and 'manoeuvres', then combinations of 'manoeuvres' to give typical flight profiles, and finally linking typical flight sequences into a usage spectrum. Analyses, based on this work, have been undertaken to support design criteria in terms of fatigue life and crack growth.

9.5.7.7 General flight record processing & individual aircraft tracking

A very large volume of data has been processed using computer techniques over the past several years, and this has led to a refinement in the approach adopted and the types of computer used which will significantly reduce future processing costs. The availability of these data has been justified several times over the last few years during incident investigations, and the value of individual aircraft tracking in permitting correlation of fatigue crack fractographic information with individual aircraft records has provided the RAAF with a powerful tool for forecasting service cracking characteristics.

9.6 BIBLIOGRAPHY ON THE FATIGUE OF MATERIALS, COMPONENTS AND STRUCTURES

The fourth volume of this work by J.Y. Mann, covering the period 1966 to 1970, is expected to be ready for publication during 1986. It will contain nearly 7,000 citations and bring the total number of citations for all four volumes to about 23,000*.

* Volumes 1, 2 and 3 of the Bibliography covering the periods 1838-1950, 1951-1960 and 1961-1965 were published by Pergamon Press in 1970, 1978 and 1983 respectively.

9.7 REFERENCES

1. Jost, G.S. A review of Australian investigations on aeronautical fatigue during the period April 1981 to March 1983. Minutes of the 18th ICAF Conference, Toulouse, May 1983.

2. Tuller, L.T. and Oswald, G. Residual strength results for the Nomad fatigue test specimen - stub wing front spar. GAF Project Note N2/105, March 1984.

3. Cameron, M.V. Fatigue test crack and repair summary. Nomad model N22. GAF Certification Report N22-7202, Issue 2, June 1984.

4. Tuller, L.T. Modifications and replacement of the Nomad lower wing skin panel (Part No. 1A/N-09-1069). GAF Project Note N2/101, December 1982.

5. Tuller, L.T. and Garrick, P. Interim theoretical fatigue evaluation of the fin attachments, Nomad Model N22B/N24A. GAF Project Note N2/104, January 1984.

6. Sherman, D.J. The cumulative exceedance distribution for accelerations due to turbulence encountered by a CT4-A Air Trainer. Aero. Res. Labs Structures Technical Memorandum 364, August 1983.

7. Hole, B. and Brassington, P. Metallurgical examination of lower wing spar segments from a Partenavia P68B aircraft. Specialist Report No. X-12/84, Materials Evaluation Facility, Airworthiness Branch, Department of Aviation, Canberra, March 1984.

8. Hole, B. Examination of cracked and broken main landing gear torque links from Piper Aerostar aircraft. Specialist Report No. X-15/84, Materials Evaluation Facility, Airworthiness Branch, Department of Aviation, Canberra, May 1984.

9. Romeyn, A. Examination of a McCauley propeller hub failure. Specialist Report No. X-26/84, Materials Evaluation Facility, Airworthiness Branch, Department of Aviation, Canberra, November 1984.

10. Hole, B. and Hollamby, D. Examination relating to a crack in the top skin of a Bell 206B helicopter main rotor blade. Specialist Report No. X-19/84, Materials Evaluation Facility, Airworthiness Branch, Department of Aviation, Canberra, July 1984.

11. Hole, B. Examination of a tension torsion pin from a UH-12E aircraft. Lab. Note 3/69, Materials Evaluation Facility, Airworthiness Branch, Department of Aviation, Canberra, March 1984.

12. Mann, J.Y., Revill, G.W. and Lupson, W.F. Improving the fatigue performance of thick aluminium alloy bolted joints by hole cold-expansion and the use of interference-fit steel bushes. Aero. Res. Labs Structures Note 486, April 1983.

13. Mann, J.Y., Machin, A.S., Lupson, W.F. and Pell, R.A. The use of interference-fit bolts or bushes and hole cold expansion for increasing the fatigue life of thick-section aluminium alloy bolted joints. Aero. Res. Labs Structures Note 490, August 1983.

14. Mann, J.Y., Machin, A.S. and Lupson, W.F. Improving the fatigue life the Mirage IIIO wing main spar. Aero. Res. Labs Structures Report 398, January 1984.

15. Mann, J.Y., Pell, R.A. and Machin, A.S. Fatigue crack propagation in Mirage IIIO wing main spar specimens and the effects of spectrum truncation on life. Aero. Res. Labs Structures Report 405, July 1984.

16. Mann, J.Y. and Revill, G.W. A comparison of fatigue lives under a complex and a much simplified flight-by-flight testing sequence. Aero. Res. Labs Structures Technical Memorandum 388, August 1984.

17. Mann, J.Y., Machin, A.S., Lupson, W.F. and Pell, R.A. Interference-fit bolts or bushes for increasing the fatigue life of thick-section aluminium alloy bolted joints. Aluminium, vol. 60, no. 7, July 1984, pp. 515-520.

18. Mann, J.Y. and Kennedy, K.J. A case study in fatigue life extension - the main spar of RAAF Mirage IIIO wings. Mech. Engng Trans. I.E. Aust., vol. ME 10, no. 2, June 1985.

19. Mann, J.Y., Pell, R.A., Jones, R. and Heller, M. The use of adhesive-bonded rivets to lessen the reductions in fatigue life caused by rivet holes. Aero. Res. Labs Structures Report 399, March 1984.

20. Mann, J.Y.; Machin, A.S.; Lupson, W.F. and Pell, R.A. Techniques for increasing the fatigue life of thick-section aluminium alloy bolted joints. Aluminium, vol. 60, no. 7, 1984, pp. 3-8.

21. Mann, J.Y. and Jost, G.S. Stress fields associated with interference fitted and cold-expanded holes. Metals Forum, vol. 6, no. 1, 1983, pp. 43-53.

22. Jost, G.S. and Carey, R.P. Strains in an elastic plate containing an interference-fit bolt near a free edge. Aero. Res. Labs Structures Report 400, March 1984.

23. Jost, G.S. and Carey, R.P. Elastic response of a half-plane to a bonded interference-fit disc of the same material. Aero. Res. Labs Structures Report 406, July 1984.

24. Jost, G.S. Stresses in a half-plane containing either a pressurized hole or an interference-fit disc. Aero. Res. Labs Structures Report 409, July 1984.

25. Jost, G.S. and Carey, R.P. Effect of edge distance on yield initiation in a remotely loaded half-plane containing a bonded interference-fit disc of the same material. Aero. Res. Labs Structures Report 413, January 1985.

26. Carey, R.P. and Heller, M. Stresses and strains resulting from two closely-spaced interference-fit fasteners. Aero. Res. Labs Structures Report (in publication), 1985.

27. Heller, M., Paul, J., Carey, R.P. and Jones, R. Finite element analysis of problems associated with life enhancement techniques. Aero. Res. Labs Structures Report 404, June 1984.

28. Jones, R. and Heller, M. On the stress analysis of bonded inserts. Aero. Res. Labs Structures Report 407, July 1984.

29. Dentry, C.S. and Sparrow, J.G. Evaluation of the blind hole drilling method for the measurement of residual stress. Aero. Res. Labs Structures Technical Memorandum 383, July 1984.

30. Finney, J.M., Harris, F.G., Pell, R.A., Dentry, C.S. and Stefoulis, C.T. Modelling for fatigue crack growth prediction in Mirage IIIO Frame 26. Aero. Res. Labs Structures Report 401, April 1984.

31. Pinkert, R.E. Damage tolerance assessment of F-4 aircraft. MCAIR 76-015, September 1976.

32. Eidinoff, H.L. and Bell, P.D. Application of the crack closure concept to aircraft fatigue crack propagation analysis. Proc. 9th ICAF Symposium, 1977: LBF-Rep. No. TR-136, 1977.

33. Clayton, J.Q. Crack closure and overloads effects in fatigue. Fracture mechanics Technology Applied to Material Evaluation and Structure Design. Eds. G.C. Sih, N.E. Ryan and R. Jones, Martinus Nijhoff Publishers, The Netherlands, 1983, pp. 491-503.

34. Jones, R., Baker, A.A. and Callinan, R.J. Residual strength of impact damaged composites. Int. J. Fract. vol. 24, 1984, R51-52.

35. Jones, R., Broughton, W., Mousley, R.F. and Potter, T. Compression failures of damaged graphite epoxy laminates. J. Composite Structures (in press).

36. Jones, R.,Keh, K.K., Callinan, R.J. and Brown, K. Analysis of multilayer laminates using three dimensional super elements. Int. J. Num. Methods in Engng vol. 20, 1984, pp. 583-587.

37. Jones, R. and Baker, A.A. Damage tolerance of graphite epoxy composites. J. Composite Structures (in press).

38. Jones, R. and Callinan, R.J. Bonded repairs to surface flaws. Theoretical and Applied Fracture Mechanics, vol. 2, no. 1, 1984, pp. 11-27.

39. Baker, A.A. Repair of cracked or defective metallic aircraft components with advanced fibre composites - an overview of Australian work. Composite Structures, vol. 2, 1984, pp. 153-181.

40. Davidson, R.G., Ennis, B.C., Mestan, S.A., Tolan, F.C. and Morris, C.E.M. Low temperature cure of nitrile-epoxy adhesives AF126 and FM73. Mats Res. Labs Technical Report OCD 84/3, 1984.

41. Broughton, W. and Baker, A.A. Forthcoming work to be published.

42. Baker, A.A., Roberts, J.D. and Rose, L.R.F. Experimental study of overlap joint parameters relevant to the K reduction due to crack patching. Proc. 28th National SAMPE Symposium, 1983, pp. 627-639.

43. Paul, J. and Jones, R. Analysis of the double overlap fatigue specimen. Aero. Res. Labs Structures Report 402, April 1984.

44. Sparkman, J.K., Giraytys, J. and Smidt, G.J. ASDAR: A FGGE real-time data collection system. Bull. Amer. Met. Soc., vol. 62, no. 3, 1981, pp. 394-400.

45. Sherman, D.J. The Australian implementation of AMDAR/ACARS and the use of derived equivalent gust velocity as a turbulence indicator. Aero. Res. Labs Structures Technical Memorandum (in preparation) 1985.

46. Grandage, J.M. A procedure for the safe operation of an aircraft fleet in which cracks are known to exist in primary structure. Paper 2.9, 13th ICAF Symposium, Pisa, 1985.

47. van Dijk, G.M. Statistical load data processing. NLR Report MP-71007-U, April 1971.

48. Fraser, R.C. A one-pass method for counting range mean pair cycles for fatigue analysis. Aero. Res. Labs Structures Note 454, June 1979.

49. Mallinson, G.D. On the genesis of reliability models. Aero. Res. Labs Structures Report 393, July 1982.

50. Mallinson, G.D. and Graham, A.D. NERF - a computer program for the Numerical Evaluation of Reliability Functions - numerical methods and program documentation. Aero. Res. Labs Structures Report 397, September 1983.

51. Graham, A.D. and Mallinson, G.D. NERF - a computer program for the Numerical Evaluation of Reliability Functions - user manual. Aero. Res. Labs Structures Report 411, February 1984.

The following four papers* are to be published by Julius Springer in the Proceedings of the IUTAM Symposium on Probabilistic Methods in the Mechanics of Solids and Structures - held in Stockholm, June 19-21, 1984.

52.* Payne, A.O., Mallinson, G.D. and Graham, A.D. Reliability approach to structural safety and safety criteria.

53.* Hasofer, A.M. A matrix-valued Weibull distribution.

54.* Leicester, R.C. Closed form solutions for cost optimised reliability.

55.* Ford, D.G. Fatigue life distribution for structures with interacting failures.

56. Scott, I.G. Monitoring crack growth during fatigue testing of aircraft by means of acoustic emission. Presented to 4th Pan Pacific Conference on NDT, Sydney, December 1983.

57. Bowles, S.J. The use of acoustic emission for detection of fatigue crack growth. Ibid.

58. Scala, C.M., Coyle, R.A. and Bowles, S.J. On the analysis of acoustic emission detected during fatigue testing of an aircraft. Proc. Rev. of Progress in Quantitiative NDE, La Jolla, California, 1984.

59. Scala, C.M. and Cousland, S.McK. Acoustic emission from the aluminium alloy 6061-T651. J. Mats Sci. Letters, vol. 3, 1984, pp. 268-270.

60. Scala, C.M. and Cousland, S.McK. Acoustic emission during fatigue crack propagation in aluminium alloy 2024- the effect of an overload. Submitted to Mat. Sci. Eng., 1984.

61. Nankivell, J.F. An evaluation of accuracies in source location using acoustic emission. Presented to 4th Pan Pacific Conference on NDT, Sydney, December 1983.

62. Martin, G.G. Acoustic emission from 4340 steel during fatigue. PhD Thesis, Monash University, Melbourne, March 1984.

63. Jost, G.S. A review of Australian investigations on aeronautical fatigue during the period April 1979 to March 1981. Minutes of the 17th ICAF Conference, Noordwijkerhout, The Netherlands, May 1981.

TABLE 9.1

SUMMARY OF MAJOR CRACKS AND REPAIRS - NOMAD FATIGUE TEST SPECIMEN

LOCATION	INITIATION POINT	DETECTED* TIME (hrs) LENGTH (mm)	HISTORY OF* CRACK	COMMENTS
Stub-Wing Rib BL 42.25 STB'D	actuator cut-out	56280 (15)	R 57630 (15) F 138006 (17)	Series of cracks formed at cut-outs for both port and starboard ribs.
Wing Stringer W STN 152 F STN 195	rivet hole securing skin	60668 (X)	R 63122 (X) R 96813 (NM) C 166500 (NM)	New cracks started, and a new repair scheme was required to cover all cracks
Upper Wing-Strut Fitting	attachment bolt hole	79837 (X)		Critical failure, fitting was replaced. No indication of crack in new fitting.
Stub-Wing Outboard Rib Port BL 50.6	bolt hole, rear spar diaphragm	81700 (40)	R 88126 (43) F 103997 (65)	Critical failure. Two similar cracks were also present. Rib was replaced.
Wing Front-Spar Doubler W STN 155	rivet hole for doubler	84420 (10)	C 166500 (49)	Crack grew to another rivet hole and stopped.
Stub-Wing Rib BL 46.9 STB'D	bolt-hole, front spar attachment	103997 (29)	F 138006 (29)	Similar to crack in port side rib.
Stub-Wing Front-Spar BL 47.7 STB'D	bolt hole for upper skin	103997 (NM)	F 138006 (16)	Critical failure, stub-wing replaced. Smaller identical crack on port side.
Stub-Wing Front-Spar Web BL 42.25	rivet hole for D-nose rib	105700 (6)	F 138006 (55)	Residual strength test performed on spar after stub-wing removal.
Stub-Wing Front-Spar Lower Cap BL 21.6 Port	rivet hole for lower skin	112581 (X)	R 112581 (X) F 138006 (NM)	Critical failure, stub-wing was removed and an external strap was fitted.
Stub-Wing Rib BL 46.9 Port	bolt hole rear spar diaphragm	125045 (10)	F 138006 (22)	Cracks in port side rib at attachment hole.
Wing Rib W STN 114	rivet hole tank bay door support	162518 (320)	C 166500 (320)	Real time of crack initiation not known. Accurate length not available until 164210 hours.
Stub-Wing Front-Spar BL 47.7 Specimen No. 2	bolt hole for upper skin	164225 (NM)	-	Critical crack. Identical to crack found in specimen No. 1.

* R - Time and length of crack at repair
F - Time and length of crack at replacement
C - Test hours and length of crack at 31 December, 1984
X - Cracked through complete cross section
NM - Not measurable accurately

TABLE 9.2

CT4-A AIR TRAINER GUST SPECTRUM

Exceedance Level (g) 0.5	0.75	1.25	1.5	Units
1.91	30.0	63.4	4.0	Exceedances/Hour
75.1	1178.8	2487.3	157.2	Exceedances/Programme

TABLE 9.3

RANGE PAIR TABLE OF ARL MIRAGE FULL-SCALE FATIGUE TEST SEQUENCE DISCRETIZED TO 14 LEVELS

LO	2	0												
	3	0	0											
	4	0	0	0										
	5	0	0	0	149									
	6	1	0	91	9523	2198								
	7	1	22	2318	21601	2805	1591							
PEAK	8	0	37	659	810	1873	1665	705						
LEVEL	9	1	18	131	575	1209	521	896	124					
	10	0	17	72	421	609	302	306	336	110				
	11	3	24	42	400	338	23	131	168	183	147			
	12	5	25	60	516	171	1	92	39	63	71	97		
	13	9	9	18	16	53	0	11	0	0	11	1	35	
HI	14	1	0	0	0	0	0	0	0	0	0	0	0	0
		1	2	3	4	5	6	7	8	9	10	11	12	13
		LO				TROUGH LEVEL								HI

TABLE 9.4

FATIGUE LIVES OF SPECIMENS UNDER ORIGINAL AND RECONSTITUTED SEQUENCES

Sequence	Log mean life (programmes) (gross-area test stress = 30.4 MPa/g)	Standard Deviation of log life
Flight-by-flight	12.13	0.048
A1	14.36	0.075
A2	13.01	0.091
R1	14.78	0.079
R2	13.2	0.080

TABLE 9.5

EPOXIDE LOSS AT DIFFERENT TEMPERATURES

Temperature, °C	Time for Consumption of Epoxide
AF 126	
80	12 h
90	5.5 h
110	70 min
120	35 min
131	23 min
FM 73	
81	6 h

TABLE 9.6

NOMINAL SHEAR STRENGTH OF ALUMINIUM-ALUMINIUM LAP SHEAR JOINTS

Cure Schedule	Shear Strength, MPa	
	20°C	80°C
AF 126		
1 h/121°C	28.4	21.3
8 h/80°C	24.6	14.0
15 h/80°C	27.4	21.3
FM 73		
1 h/121°C	39.2	30.4
8 h/80°C	37.3	27.2
15 h/80°C	38.1	30.0

TABLE 9.7

DATA FROM BOEING WEDGE-TEST EXPERIMENTS FOR 2024-T3 CLAD SPECIMENS PREPARED WITH ADHESIVES AF126 OR FM73 MADE UNDER THE CONDITIONS INDICATED

Adhesive	Cure Condition	Surface-Treatment	Pressure Method	Initial Crack Size (mm)	Crack growth in given hours (mm) 2	4	24	48
AF 126	80°C/8h	An	M	30	2.8	3.5	7.0	9.4
		An	V	35	2.3	3.7	7.0	8.8
		An + S	M	36	1.7	2.3	2.9	3.4
	100°C/4h	An	M	30	0.9	1.2	2.2	2.4
		An	V	35	2.0	2.6	4.4	4.6
		An + S	M	30	1.1	1.6	2.9	3.8
	120°C/1h	An	M	29	0.9	1.3	2.8	3.4
		An	V	35	1.0	2.2	2.8	3.4
		An + S	M	27	1.4	1.5	2.1	2.6
		GB	M	28	15.0	19.0	23.0	43.0
		GB + S	M	27	20.0	2.9	7.0	8.7
FM 73	80°C/8h	An	M	37	8.7	19.0	27.0	33.0
		An	V	39	12.5	18.0	29.0	32.0
		An + S	M	38	1.1	1.4	2.3	2.9
		GB + S	M	40	10.0	1.4	2.6	3.3
	100°C/4h	An	M	36	2.1	3.8	12.0	18.0
		An	V	36	4.0	6.8	17.5	19.4
		An + S	M	36	0.2	0.5	2.0	2.4
		GB + S	M	37	0.7	0.9	1.4	1.6
	120°C/1h	An	M	36	1.7	1.8	6.8	9.6
		An	V	34	1.7	2.2	11.0	15.5
		An + S	M	34	1.2	1.5	2.4	2.6
		GB	M	28	15.2	18.7	33.2	42.6
		GB + S	M	35	0.4	0.8		1.4

Notation

An PANTA
GB grit-blast
S silane prime
M mechanical pressurization
V vacuum bag pressurization

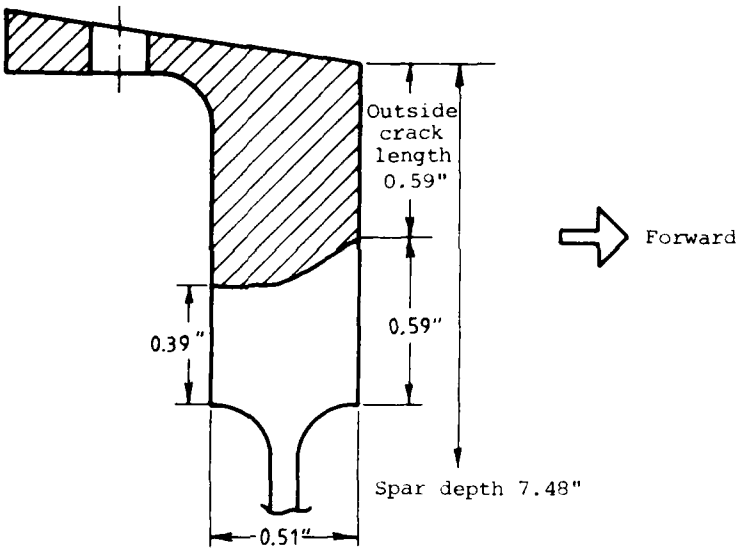

FIG. 9.1 CROSS-SECTION OF NOMAD STUB WING UPPER-SPAR-CAP CRACK (B.L.47.6)

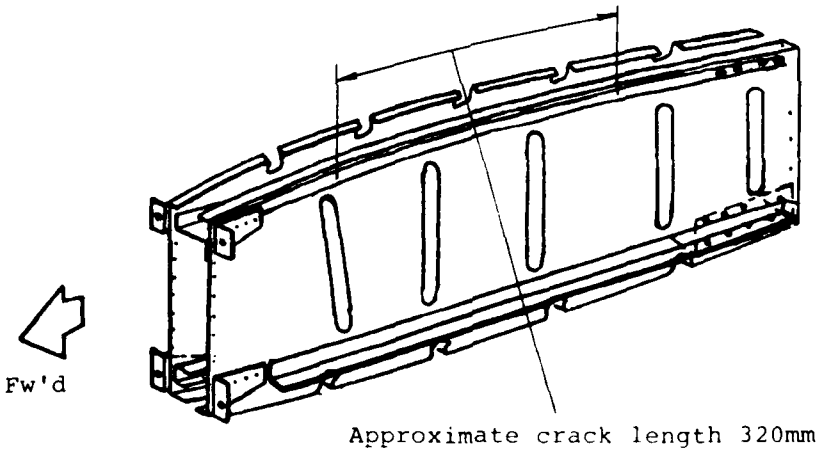

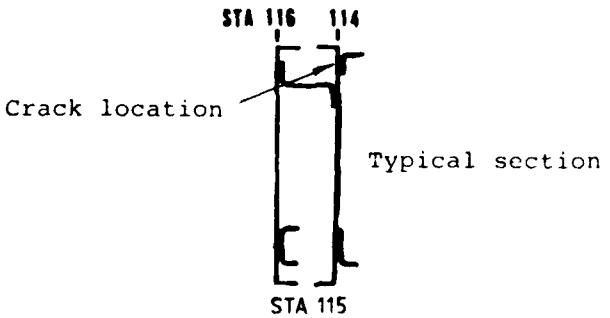

FIG. 9.2 NOMAD WING RIB ASSEMBLY SHOWING LOCATION OF CRACKING ON FATIGUE TEST

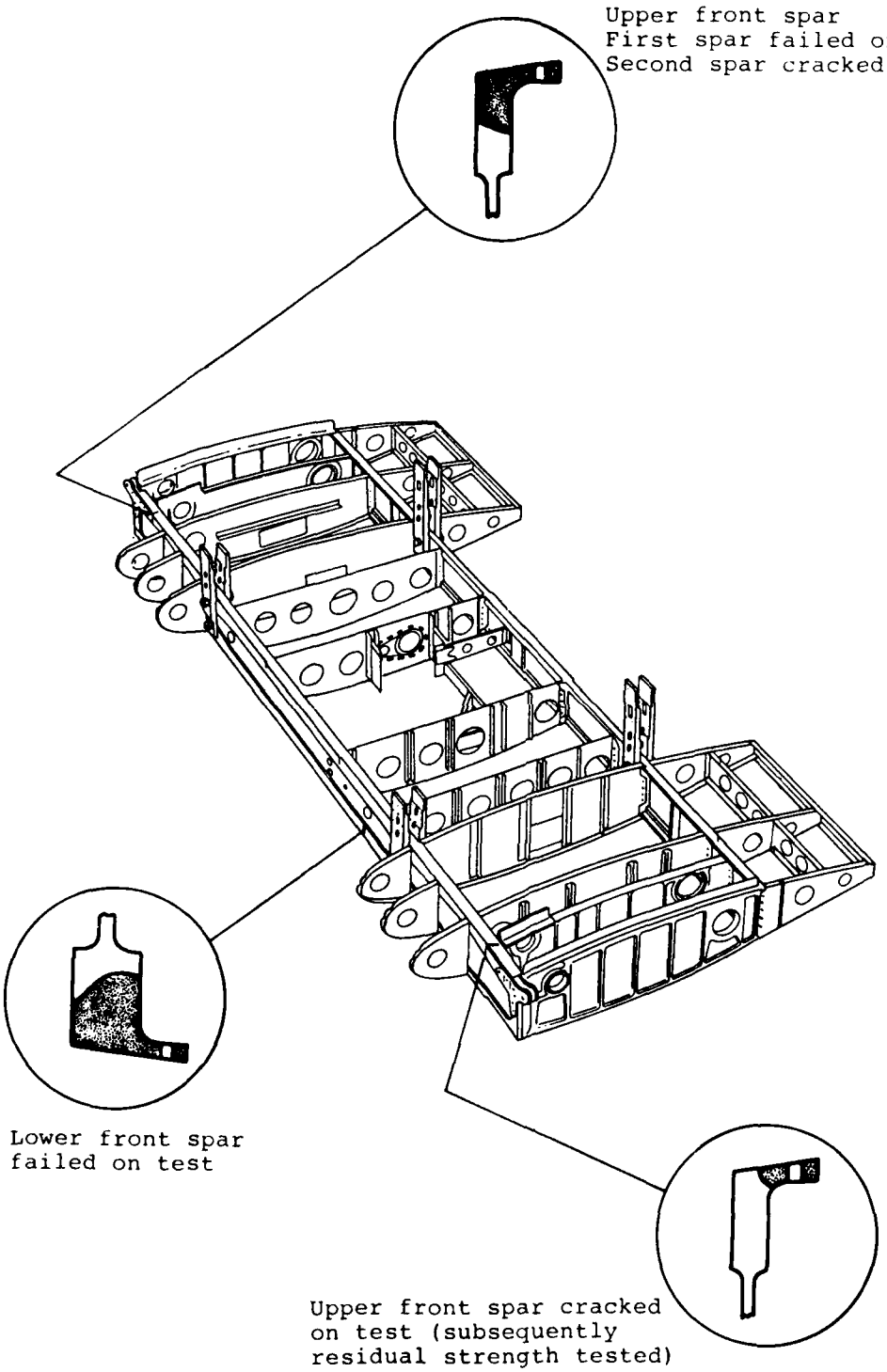

FIG. 9.3 NOMAD STUB WING SHOWING LOCATIONS OF MAJOR FATIGUE TEST FAILURES

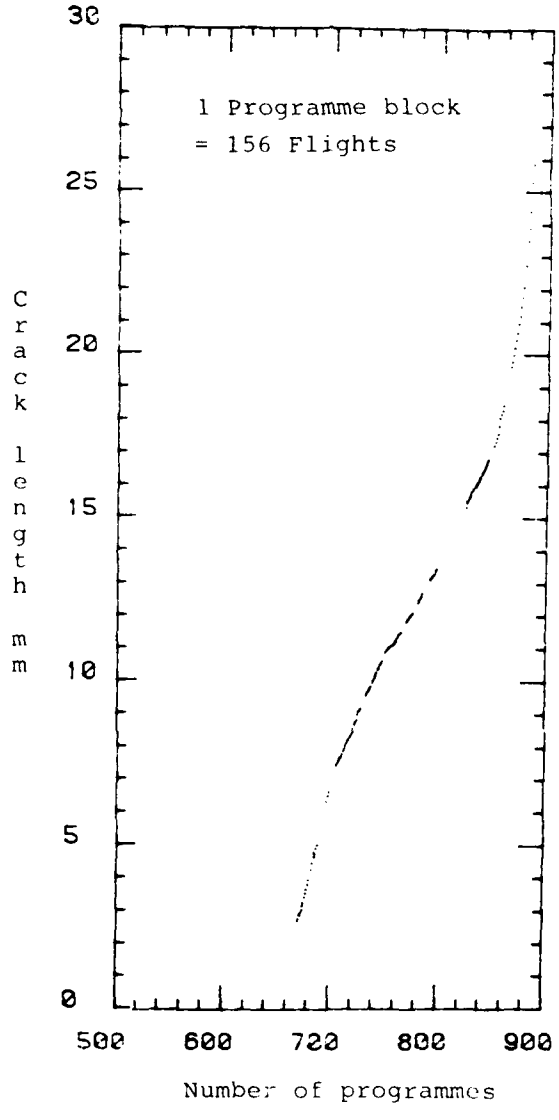

FIG. 9.4 RADIAL CRACK DEPTH VERSUS THE NUMBER OF PROGRAMME BLOCKS FOR THE NOMAD STUB WING FRONT SPAR UPPER CAP FAILURE AT B.L. 47.6

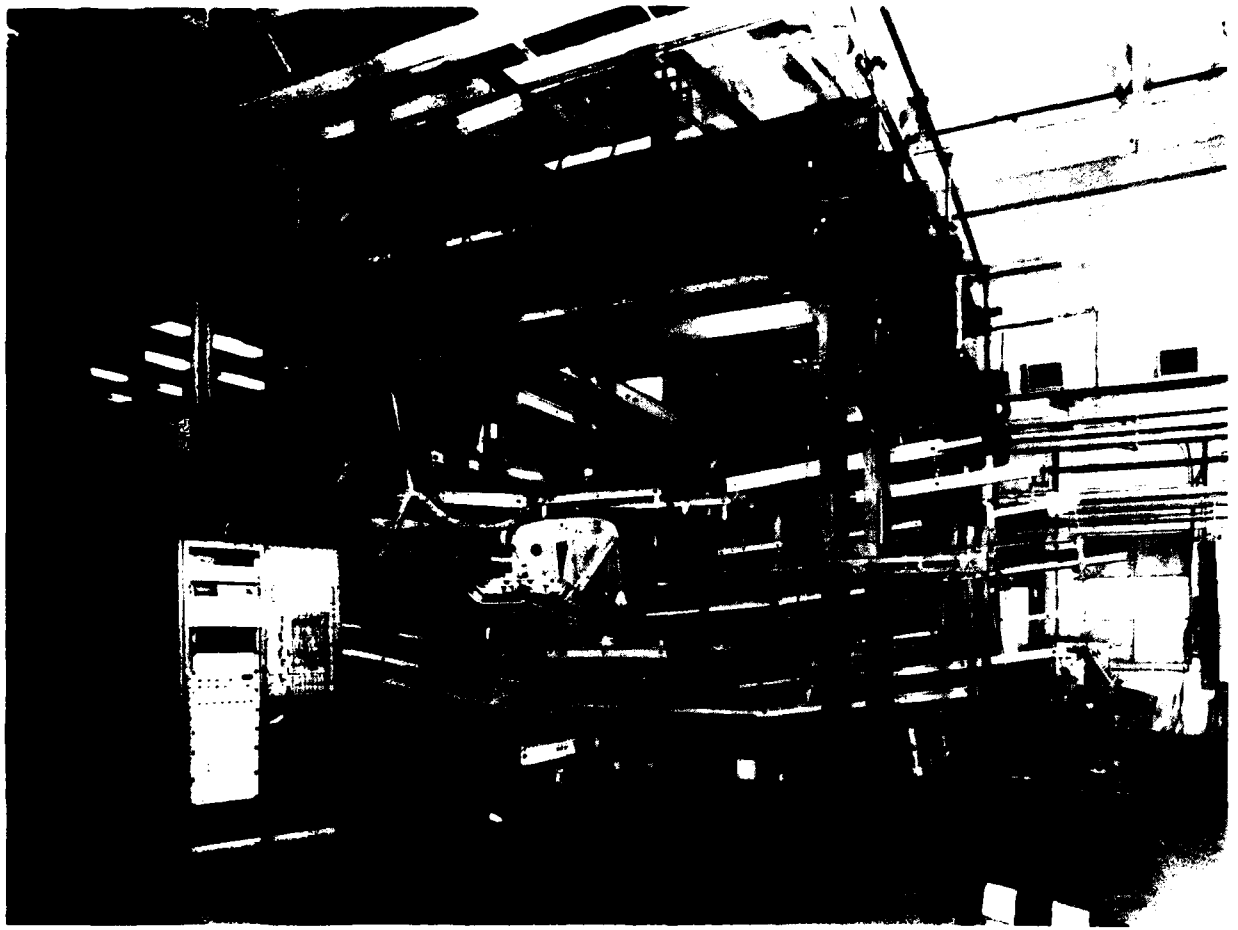

FIG. 9.5 CT4-A FULL-SCALE FATIGUE TEST

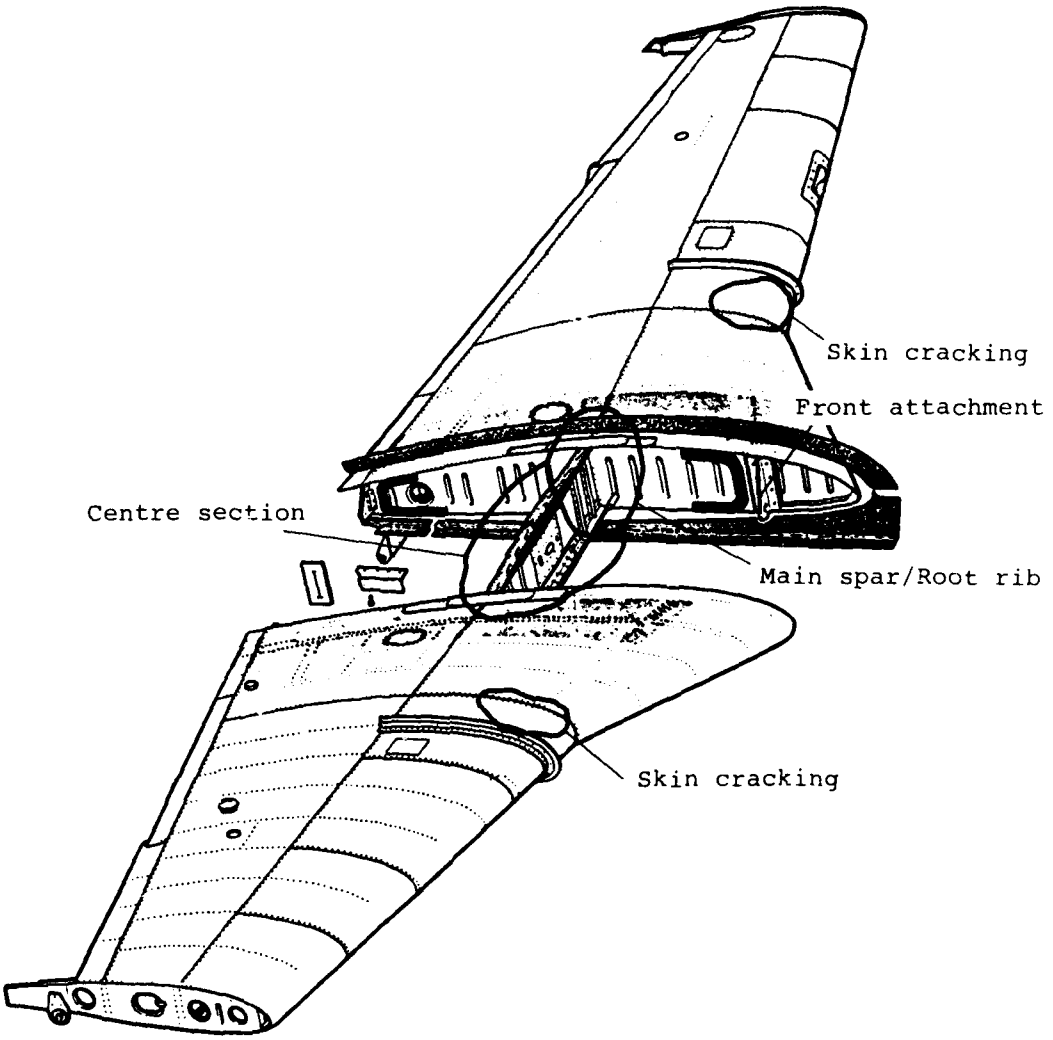

FIG. 9.6 CT4-A MAIN PLANE ASSEMBLY

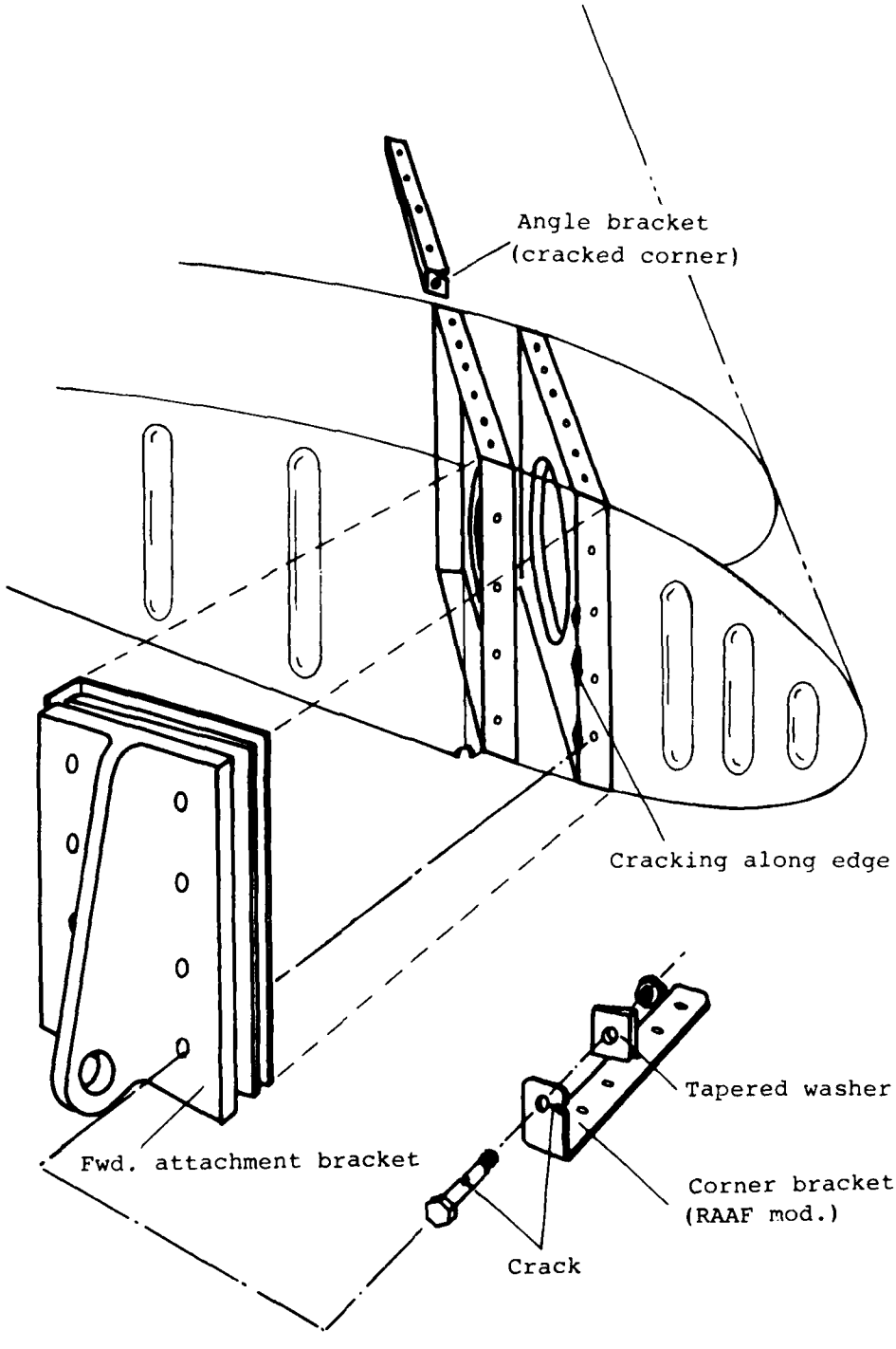

FIG. 9.7 CT4-A FORWARD WING ATTACHMENT DETAILS SHOWING DAMAGE AT 5000 HRS.

FIG. 9.8 CT4-A UPPER SURFACE BUCKLING SHOWING STANDARD PATCH REPAIR - STARBOARD WING

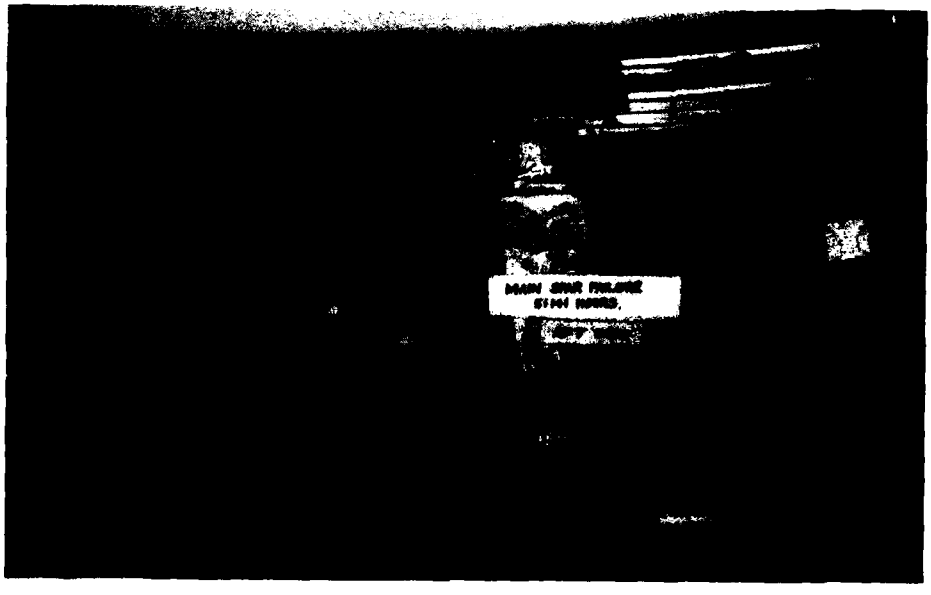

FIG. 9.9 CT4-A MAIN SPAR FAILURE - PORT WING

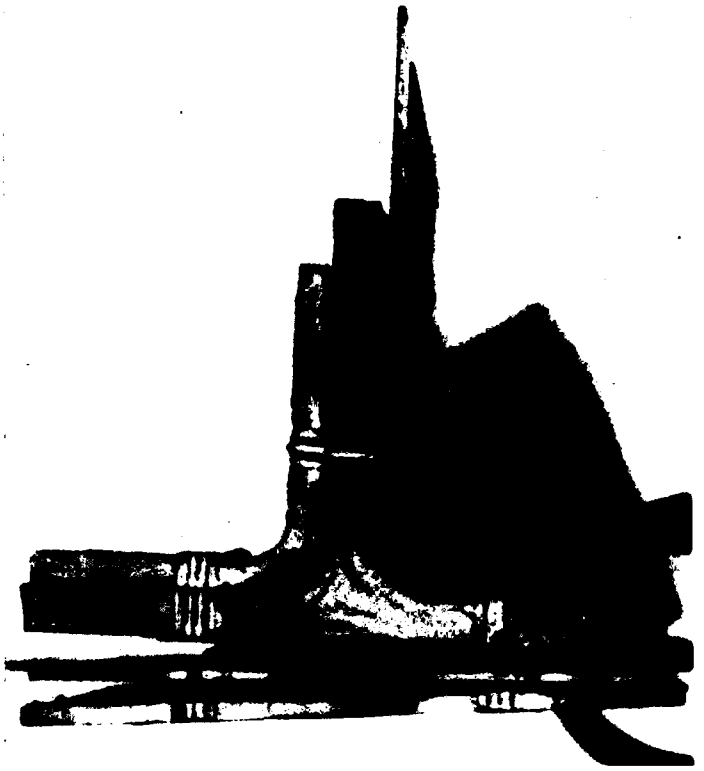

FIG. 9.10

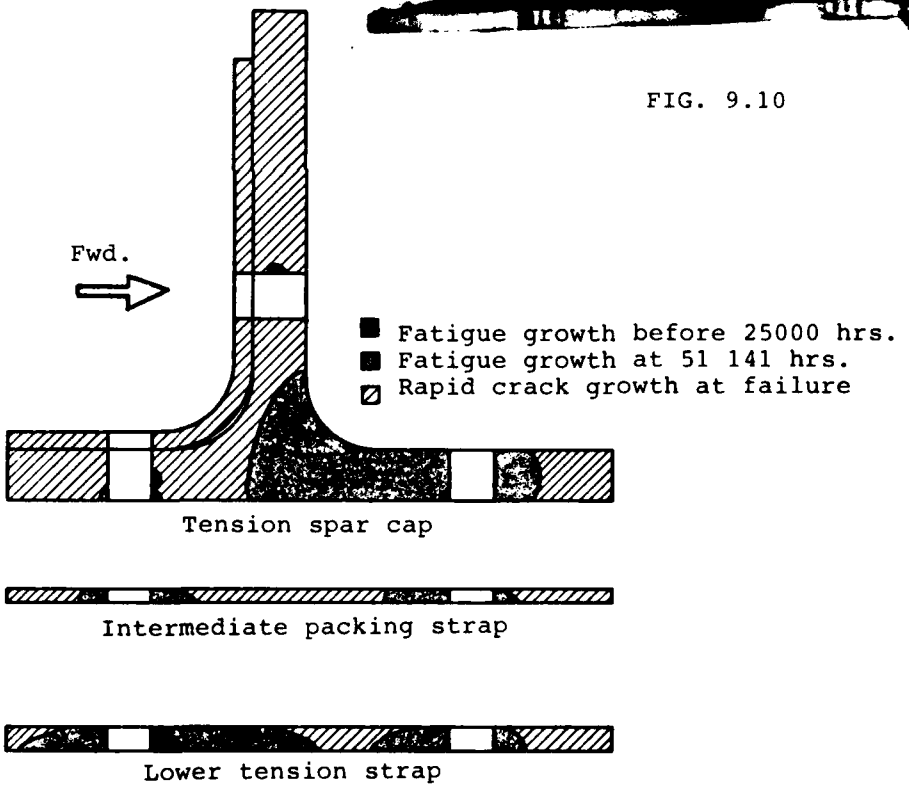

FIG. 9.11 CT4-A MAIN SPAR TENSION BOOM FAILURE

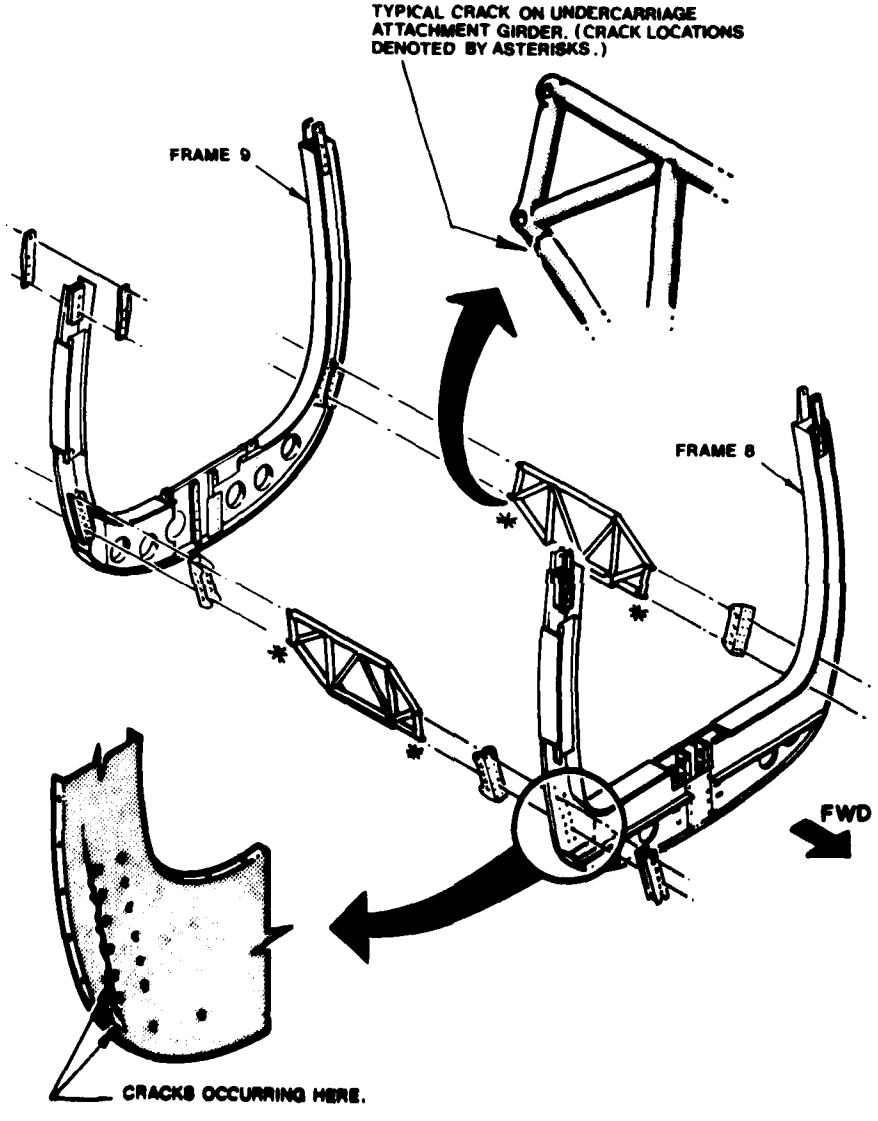

FIG. 9.12 PARTENAVIA P68 CENTRE FUSELAGE STRUCTURE SHOWING CRACKED FRAMES

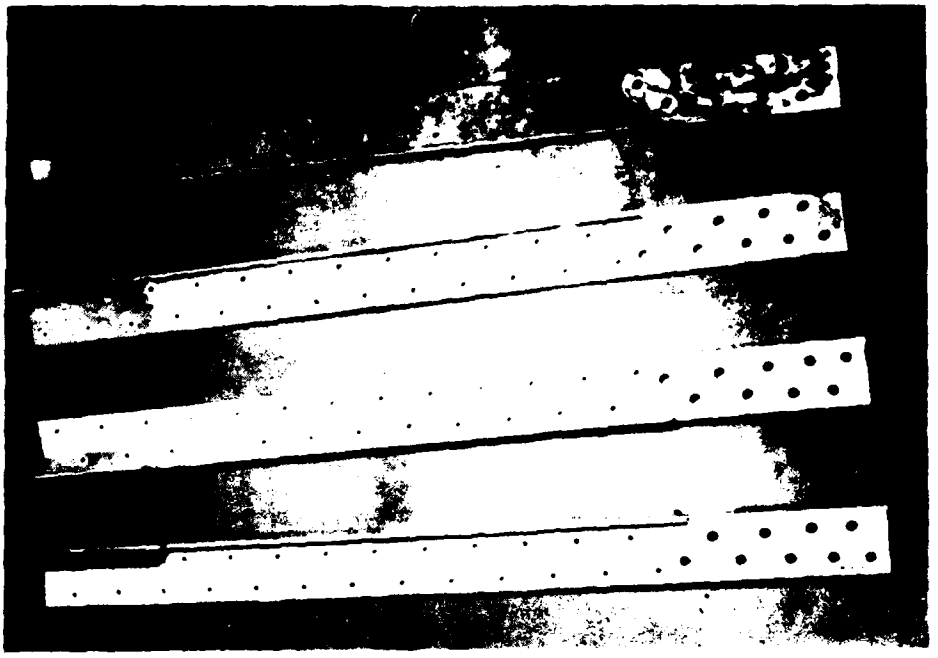

FIG. 9.13 PARTENAVIA P68 FRONT SPAR FORWARD AND AFT LOWER CAP ANGLES, AS REMOVED

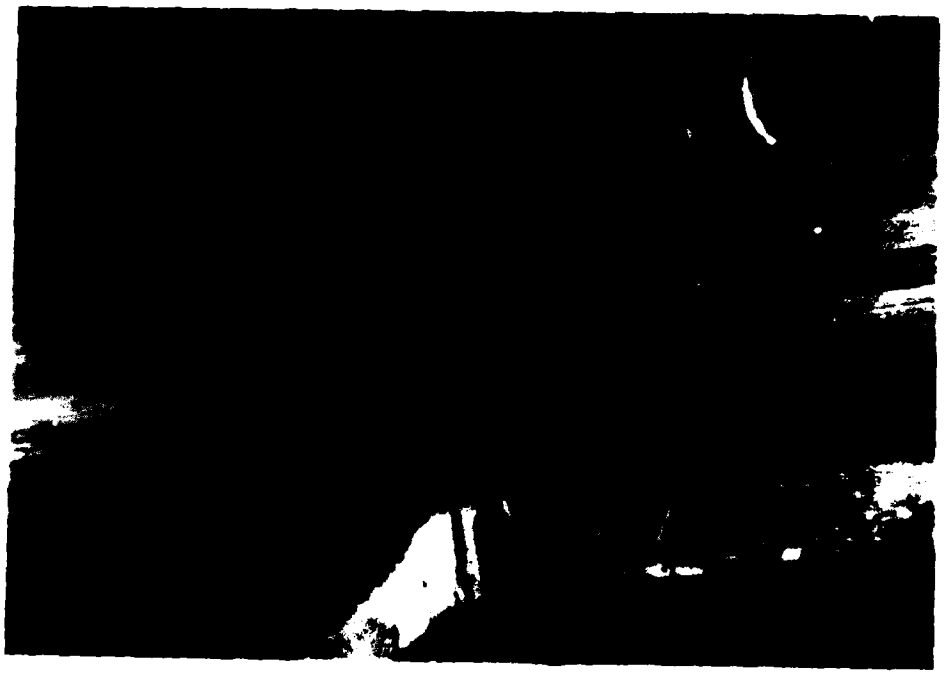

FIG. 9.14 CRACK IN PARTENAVIA P68 SPAR SHOWING ABRUPT CHANGE IN SECTION, SMALL RADIUS AND POOR SURFACE FINISH (x 3 approx.)

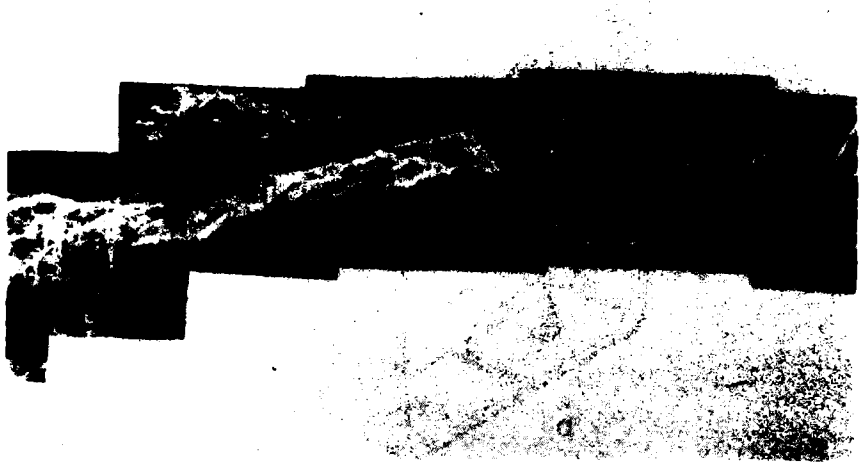

FIG. 9.15 PARTENAVIA P68 FRONT SPAR CRACKING:
PHOTO-MOSAIC OF PART OF FRACTURE SURFACE

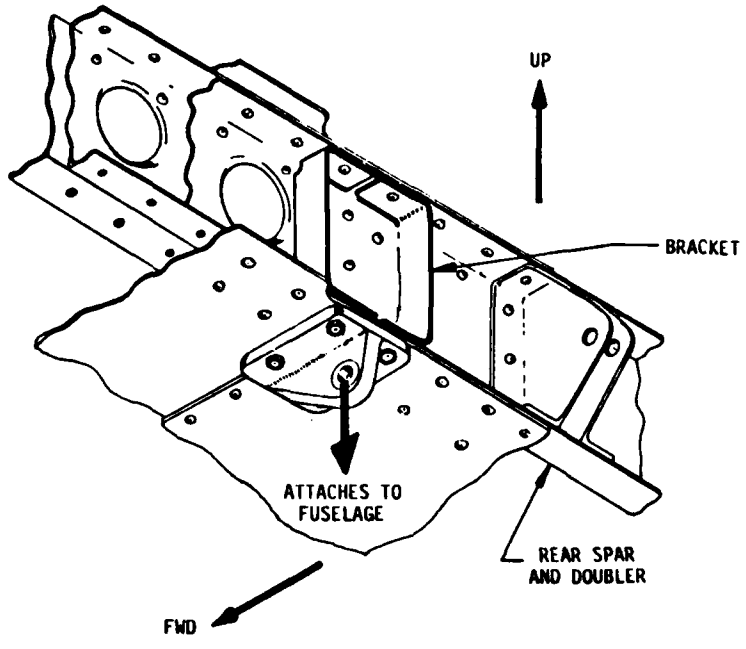

FIG. 9.16 CESSNA 210 TAILPLANE BRACKET INSTALLATION
(LEFT SIDE ONLY SHOWN)

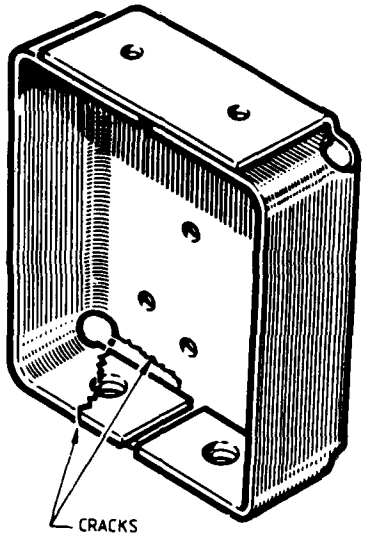

FIG. 9.17 CESSNA 210 TAILPLANE REAR SPAR REINFORCEMENT BRACKET

FIG. 9.18 FRACTURE SURFACE OF CESSNA 210 TAILPLANE REINFORCING BRACKET SHOWING MULTIPLE CRACK ORIGINS

FIG. 9.19 CRACKED AND BROKEN MAIN LANDING GEAR TORQUE LINKS FROM PIPER AEROSTAR 600

FIG. 9.20 PIPER AEROSTAR 600: FRACTURE SURFACE OF FAILED TORQUE SHOWING AREAS OF FATIGUE (F) AND OVERLOAD (O) x 7.3 approx.

FIG. 9.21 McCAULEY D3A 32C90-LM PROPELLER HUB AS RECEIVED

FIG. 9.22 McCAULEY D3A 32C90-LM FRACTURE SURFACE, MULTIPLE ORIGINS

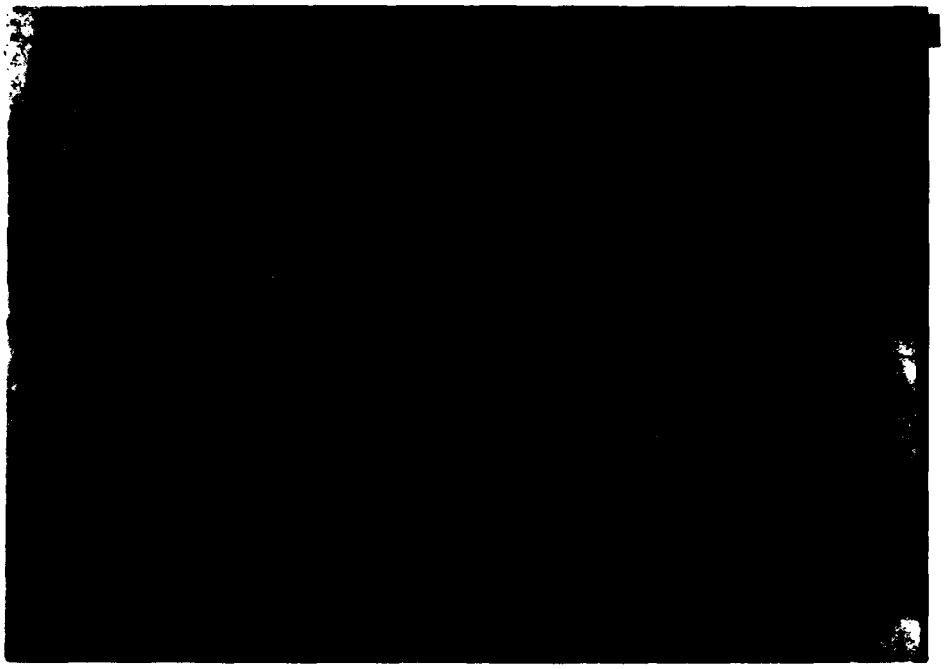

(x340 Approx)

FIG. 9.23 SECTION THROUGH RETENTION THREAD ROOT SHOWING SURFACE FINISH - McCAULEY D3A 32C90-LM

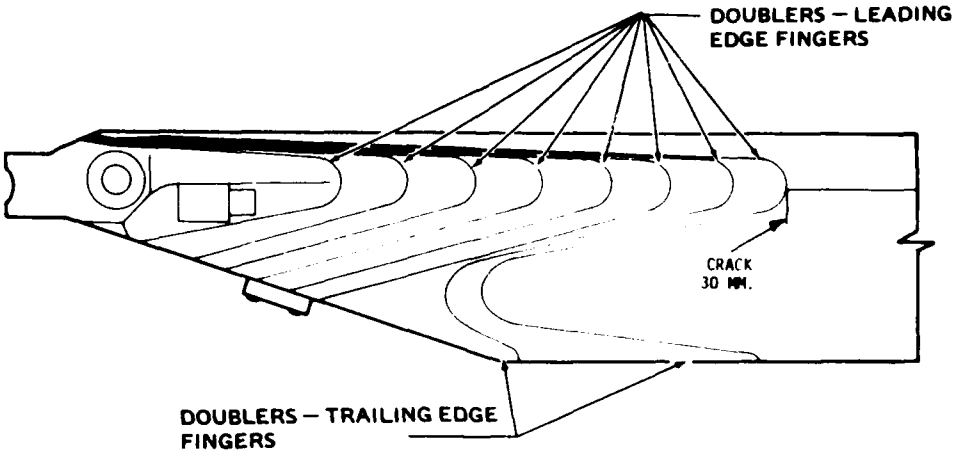

FIG. 9.24 BELL 206 B MAIN ROTOR BLADE REINFORCEMENT

FIG. 9.25 BELL 206 B MAIN ROTOR BLADE - ROOT END SKIN CRACK

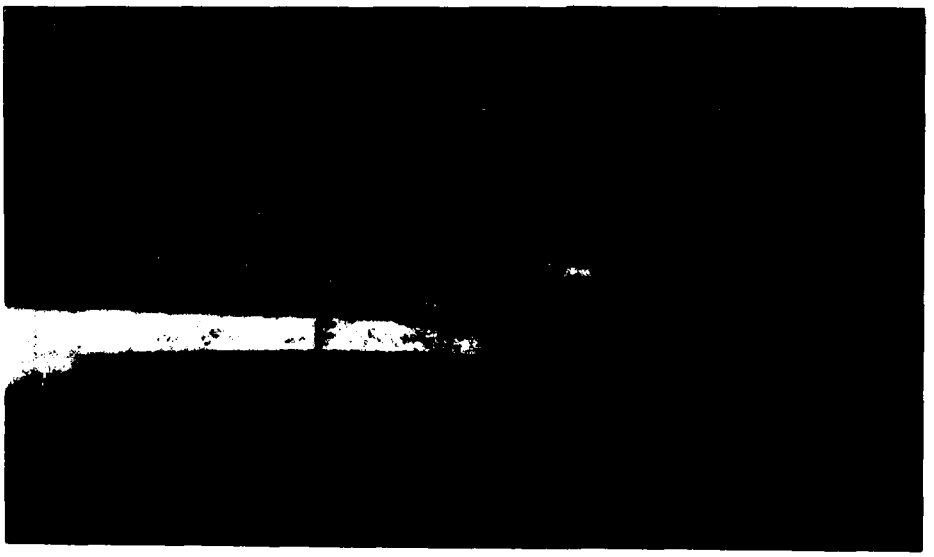

FIG. 9.26 BELL 206 B MAIN ROTOR BLADE FRACTURE SURFACE SHOWING REDUCED THICKNESS OF BLADE SKIN AT CRACK INITIATION SITE. FRACTURE SURFACE IS MARKED (F)

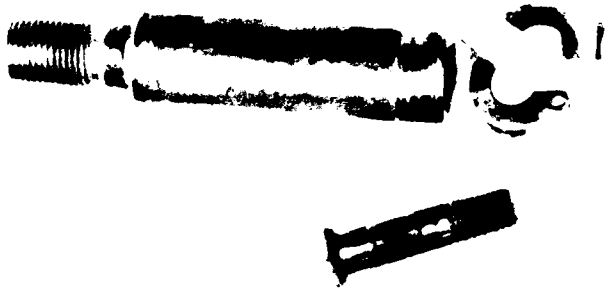

FIG. 9.27 BROKEN HILLER UH-12E DRAG LINK ATTACHMENT SHOWING CORROSION, WEAR AND FRETTING ON PIN AND THROUGH BOLT.

FIG. 9.28 FATIGUE FRACTURE SURFACE OF HILLER UH-12E EYE BOLT END SHOWING MULTIPLE ORIGINS, WITH CORROSION AND FRETTING IN BOLT HOLE BORE

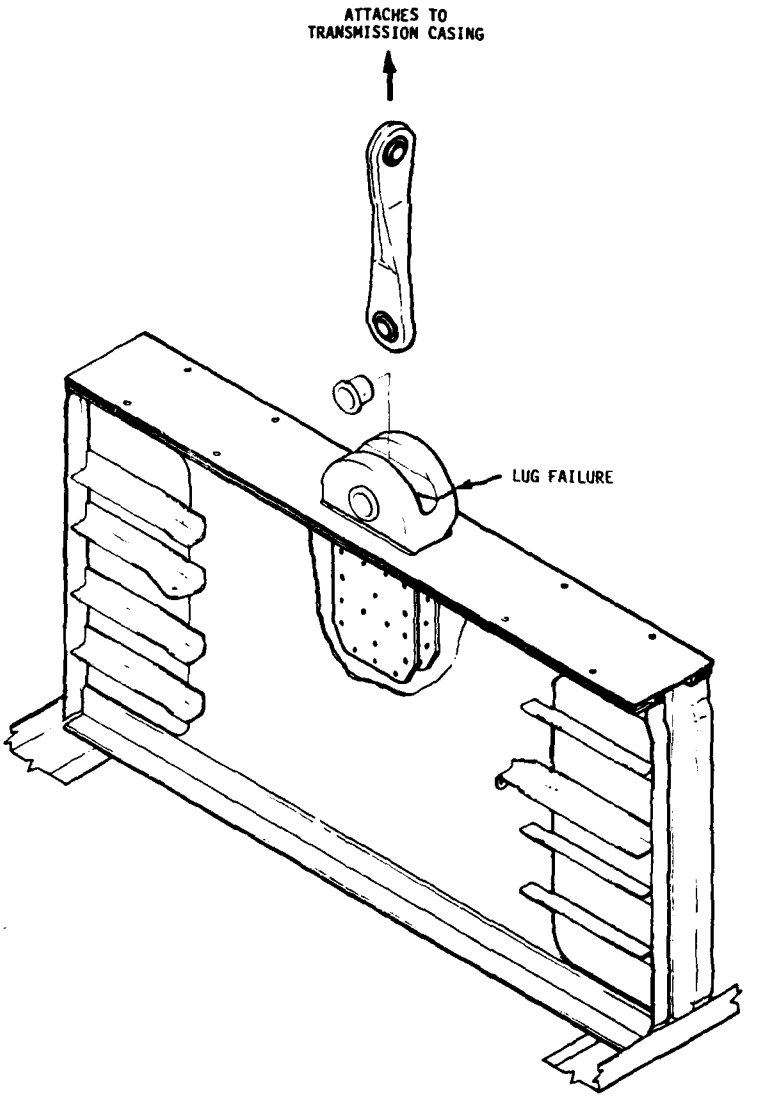

FIG. 9.29 LIFT LINK, LIFT BEAM AND ATTACHMENT FITTING - BELL 212 HELICOPTER

FIG. 9.30 BELL 212 HELICOPTER, LIFT LINK LOWER ATTACHMENT FITTING - FRACTURE SURFACE

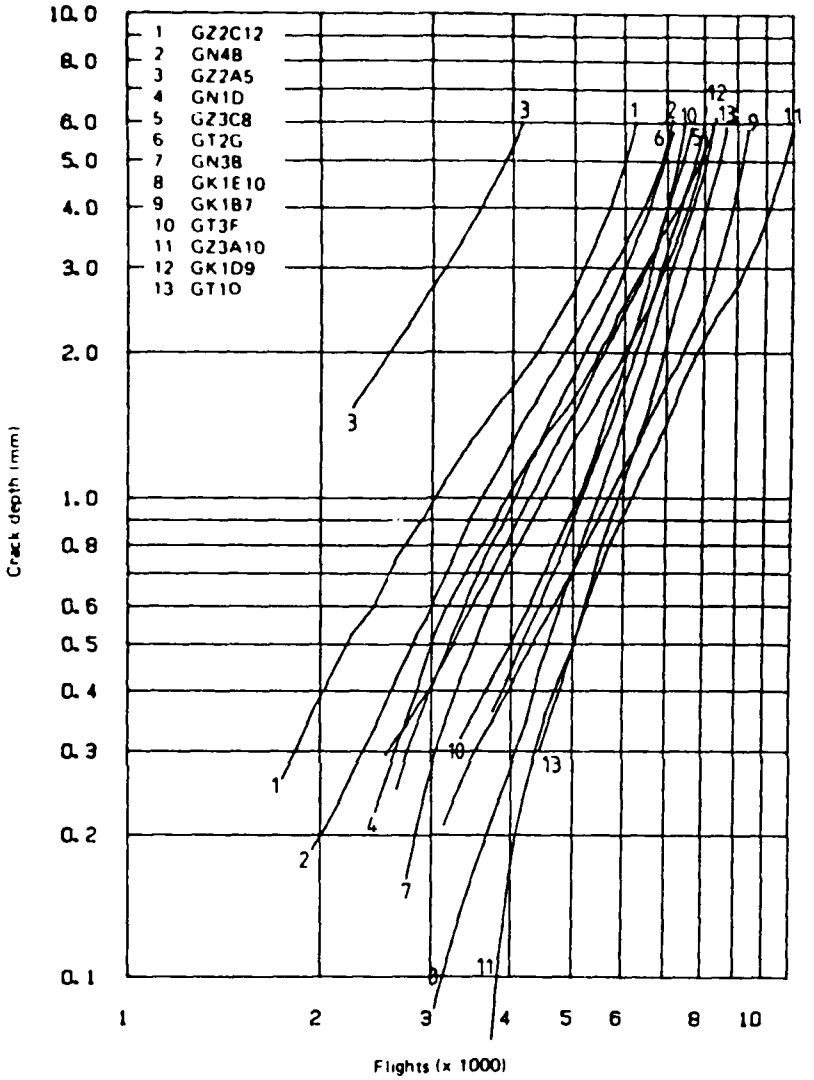

FIG. 9.31 FATIGUE CRACK GROWTH FROM 8mm BOLT HOLE
SPECIMENS WITH 0.125 INCH SLAN RIVETS, SPECTRUM TYPE 1

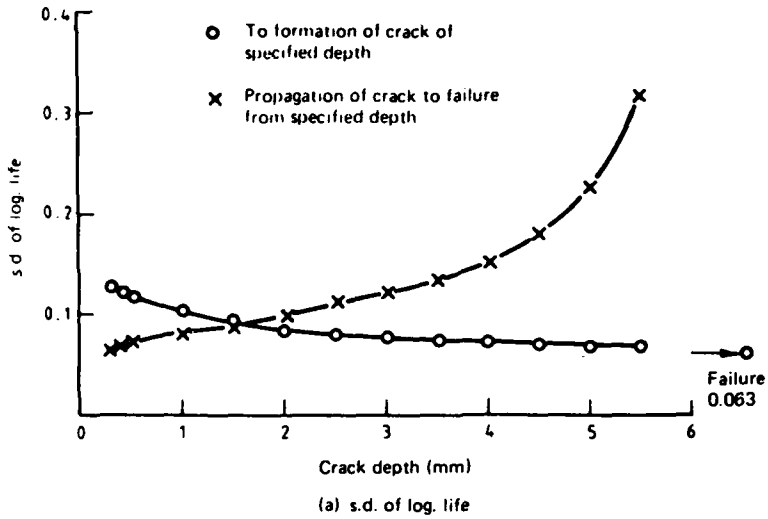

(a) s.d. of log. life

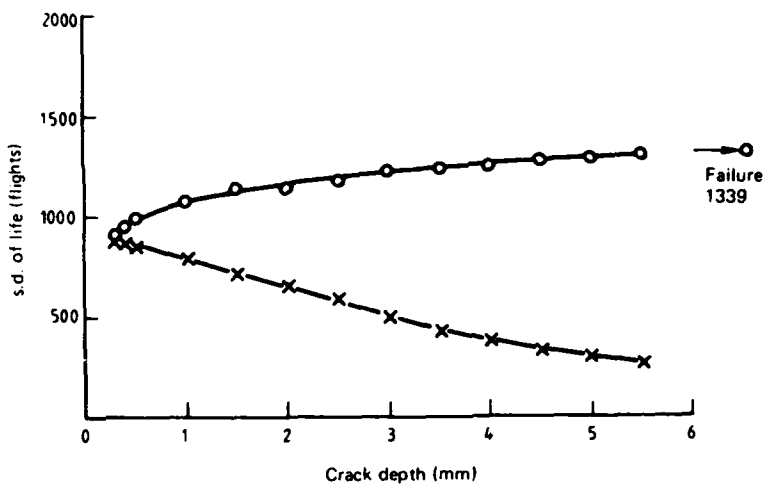

(b) Arithmetic s.d. of lives

FIG. 9.32 VARIABILITY IN LIVES TO FORMATION AND PROPAGATION OF CRACKS OF SPECIFIED DEPTHS

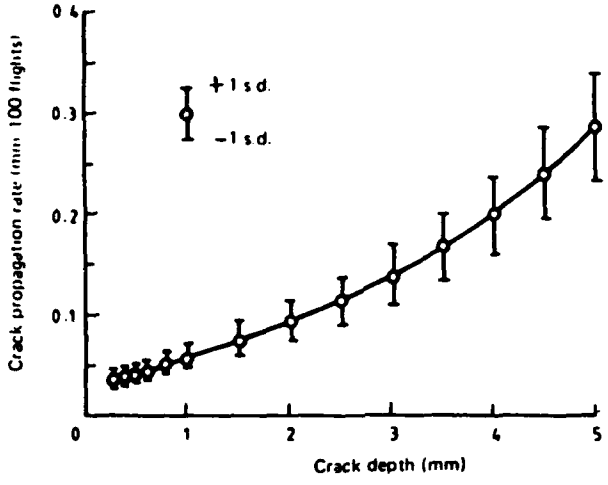

(a) Crack propagation rates

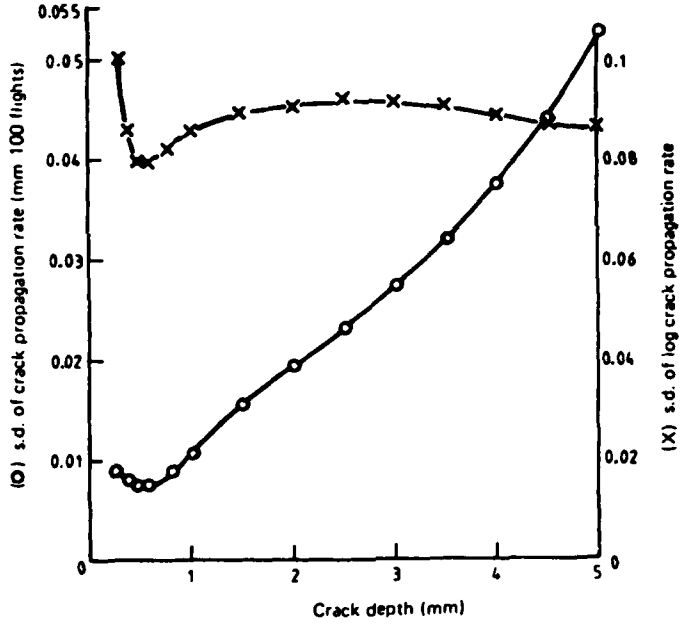

(b) s.d. of crack propagation rates

FIG. 9.33 RELATIONSHIPS BETWEEN CRACK PROPAGATION RATES AND CRACK DEPTHS

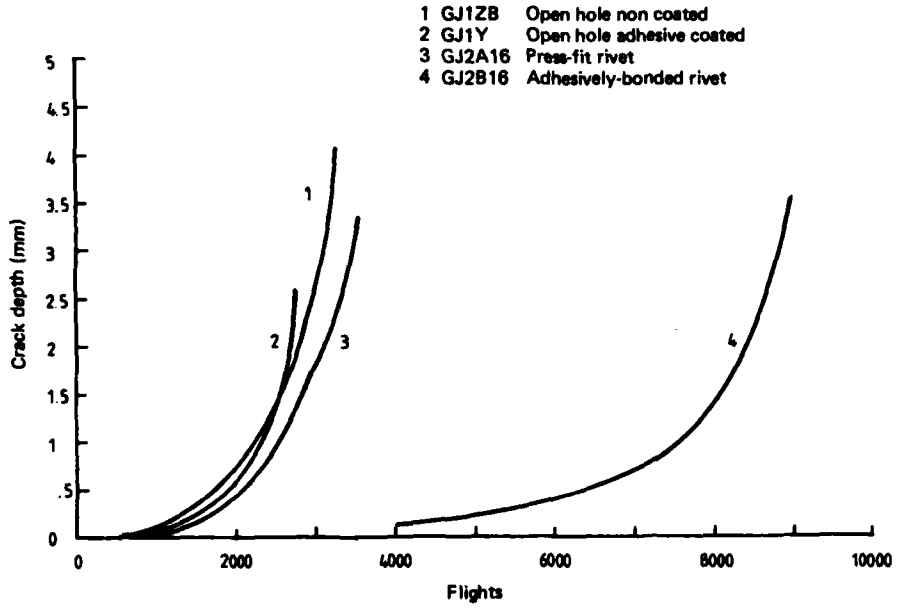

FIG. 9.34 EFFECT OF ADHESIVE BONDING ON CRACK PROPAGATION

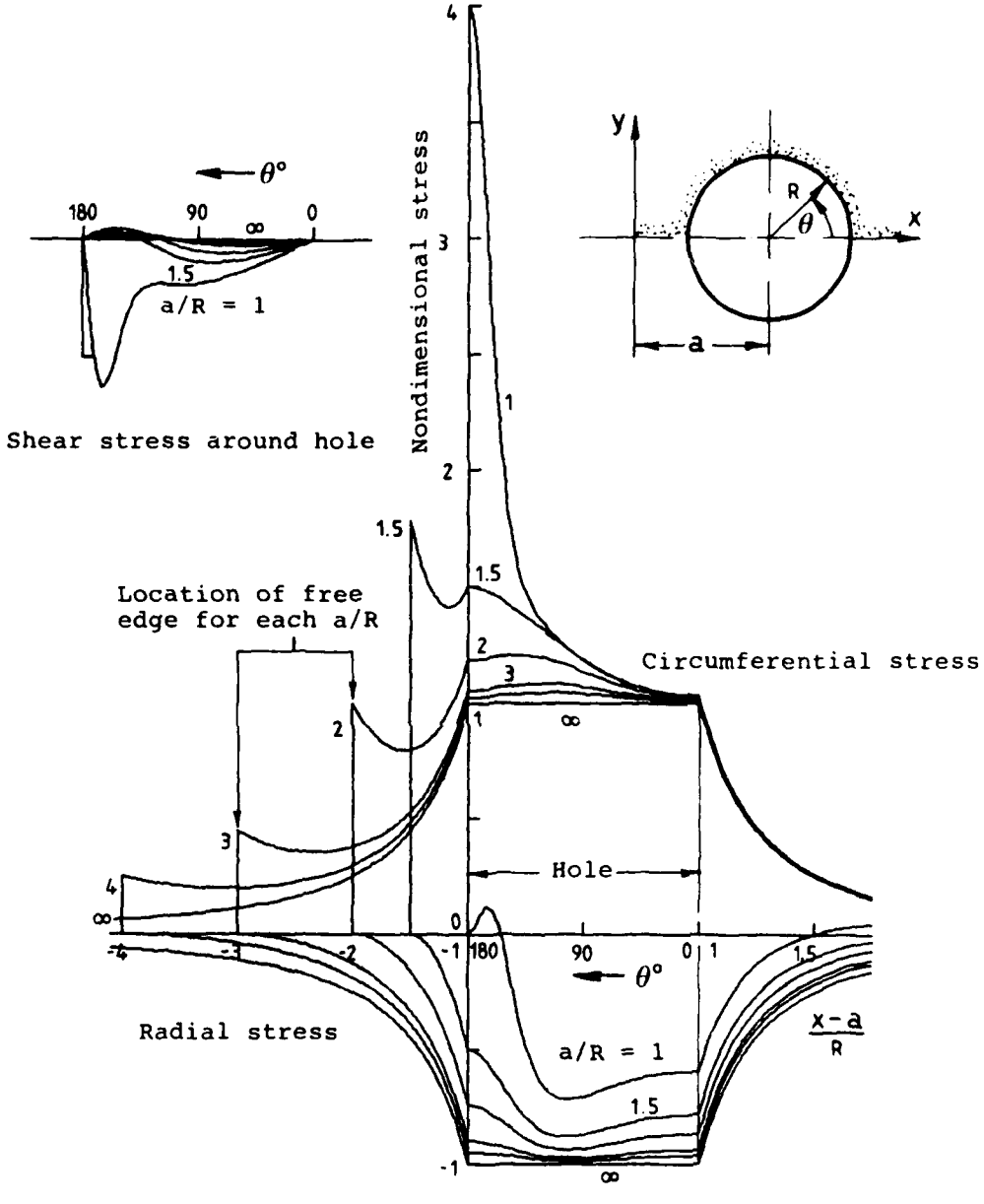

FIG. 9.35 ELASTIC INTERFERENCE-FIT STRESS DISTRIBUTION AROUND HOLE AND ALONG X AXIS - EFFECT OF EDGE DISTANCE

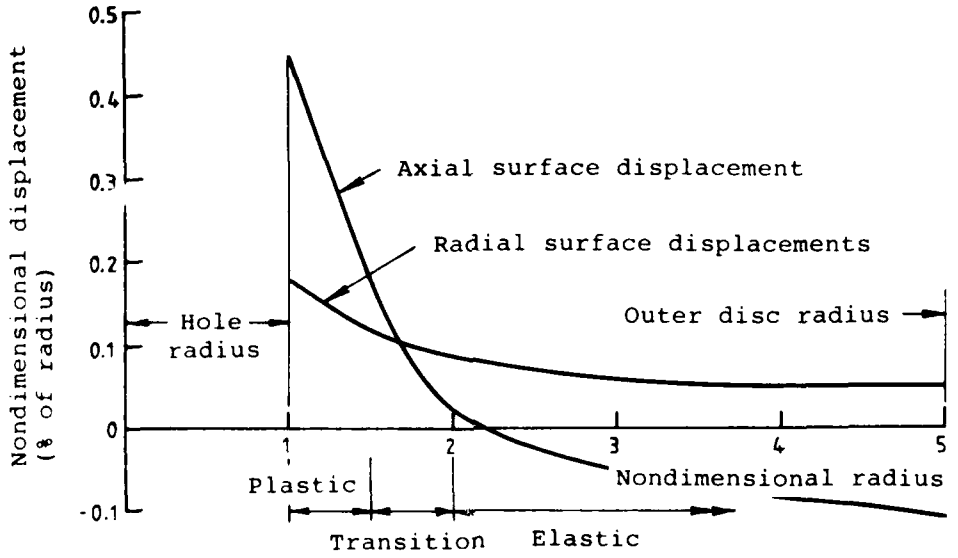

FIG. 9.36 SURFACE DISPLACEMENT OF AN ALUMINIUM ALLOY DISC CONTAINING A PRESSURIZED HOLE (NONDIMENSIONAL THICKNESS = 6.25)

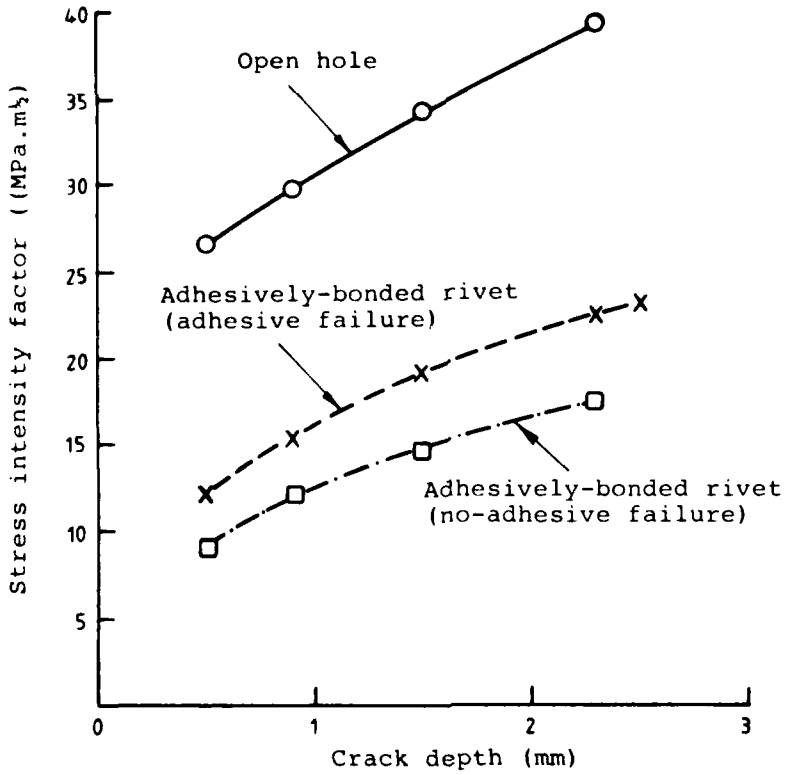

FIG. 9.37 STRESS INTENSITY FACTORS FOR HOLES WITH CRACKS ON BOTH SIDES

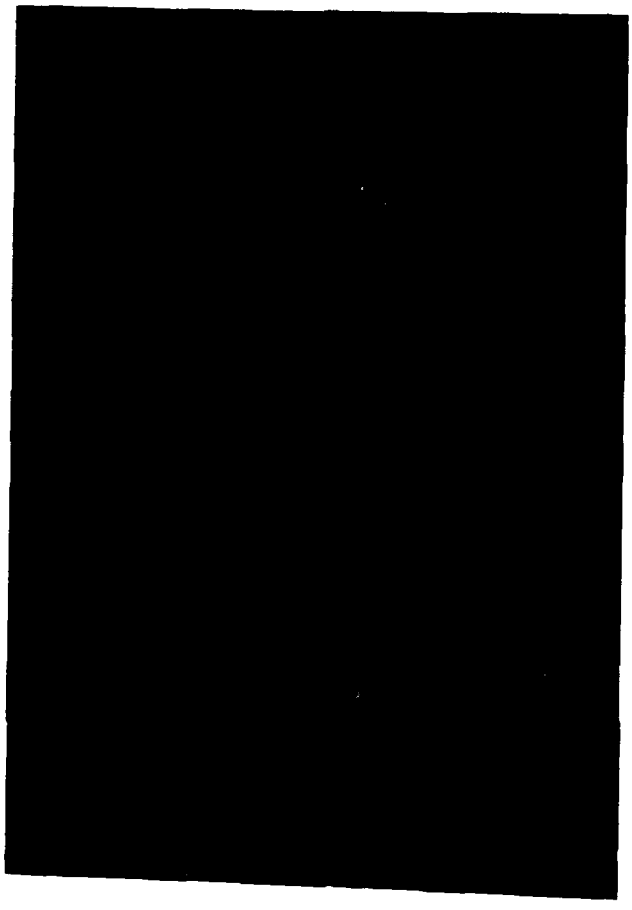

FIG. 9.38 PHOTOELASTIC FRINGE PATTERNS AT MANDREL ENTRY (TOP) AND EXIT SIDE OF A COLD EXPANDED HOLE - SPLIT SLEEVE

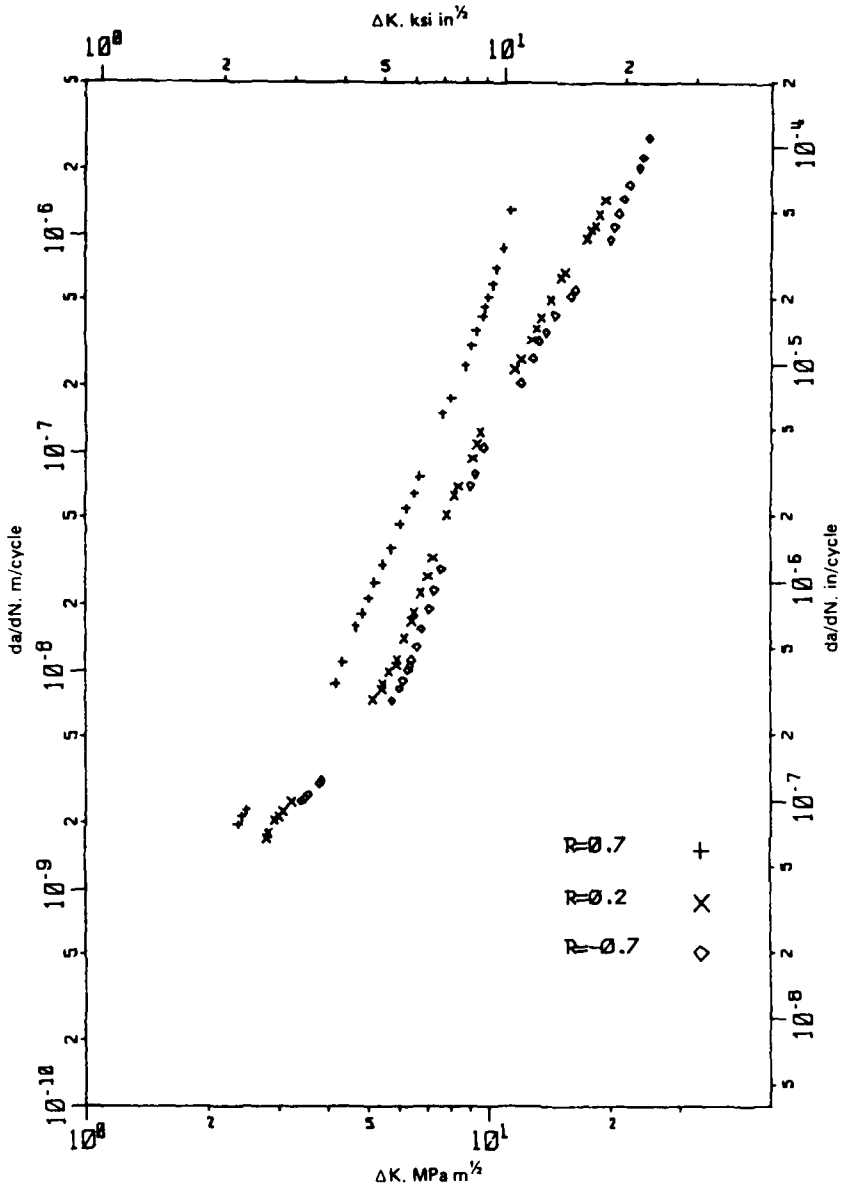

FIG. 9.39 CRACK GROWTH DATA FOR 20mm THICK CCT SPECIMENS

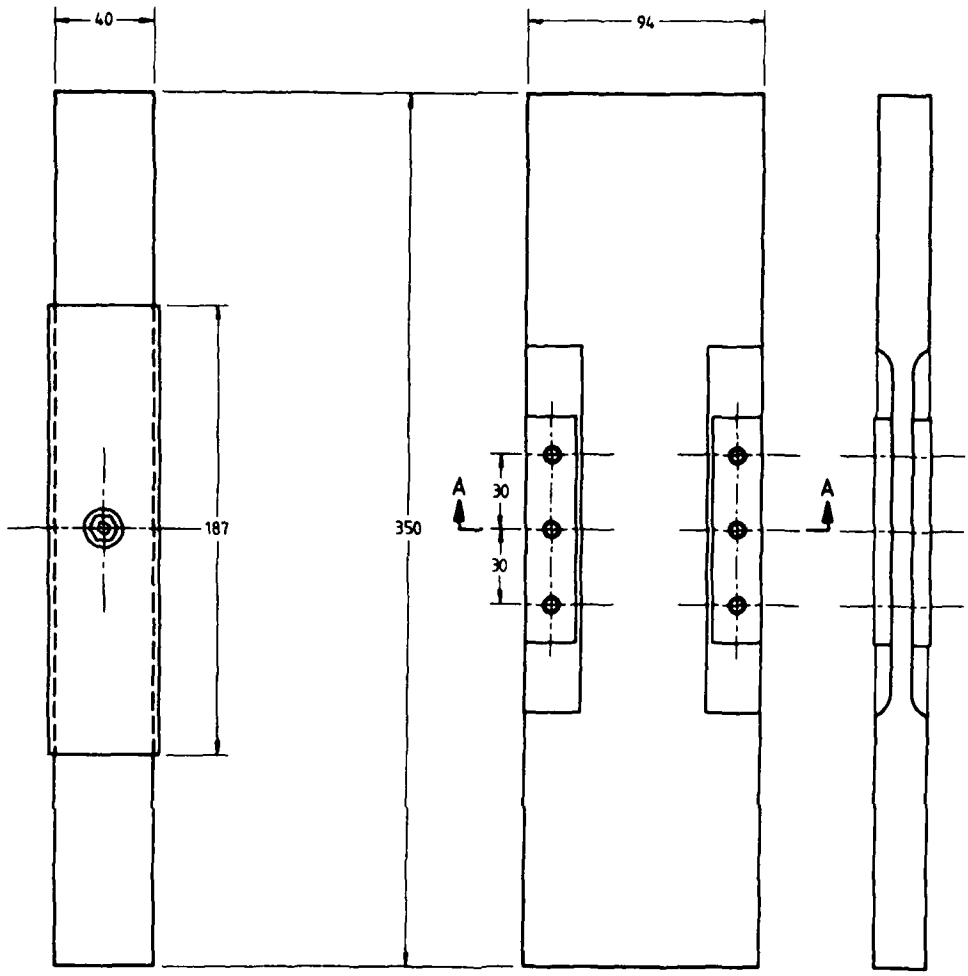

FIG. 9.40 HOLE 18

FIG. 9.41 BOTTOM OF FRAME

Simulation specimens for regions of
Mirage Frame 26

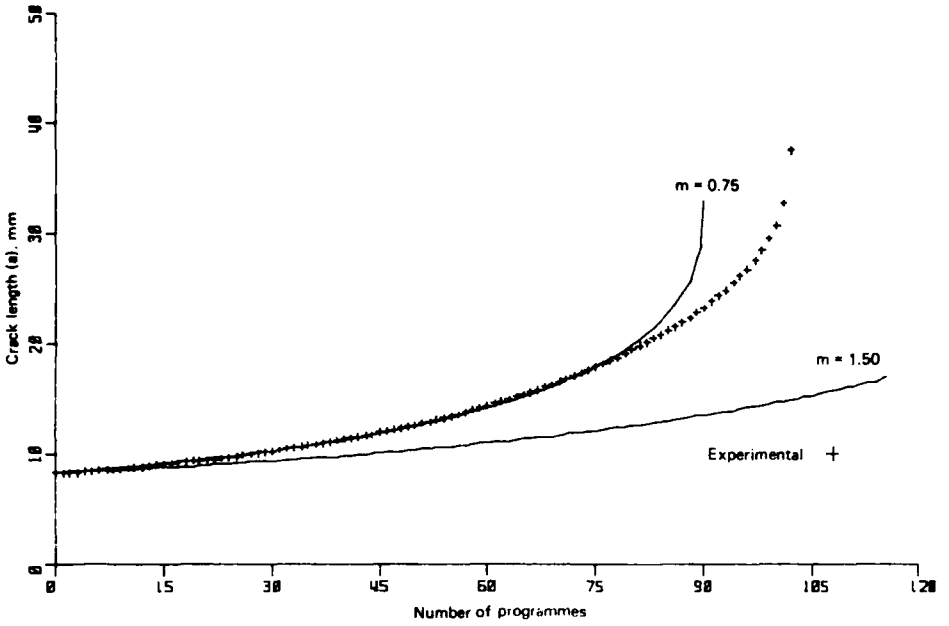

FIG. 9.42 CALIBRATION OF WHEELER EXPONENT, m. 20mm THICK CCP SPECIMEN TESTED UNDER THE F + W SEQUENCE (13.33 MPa/g)

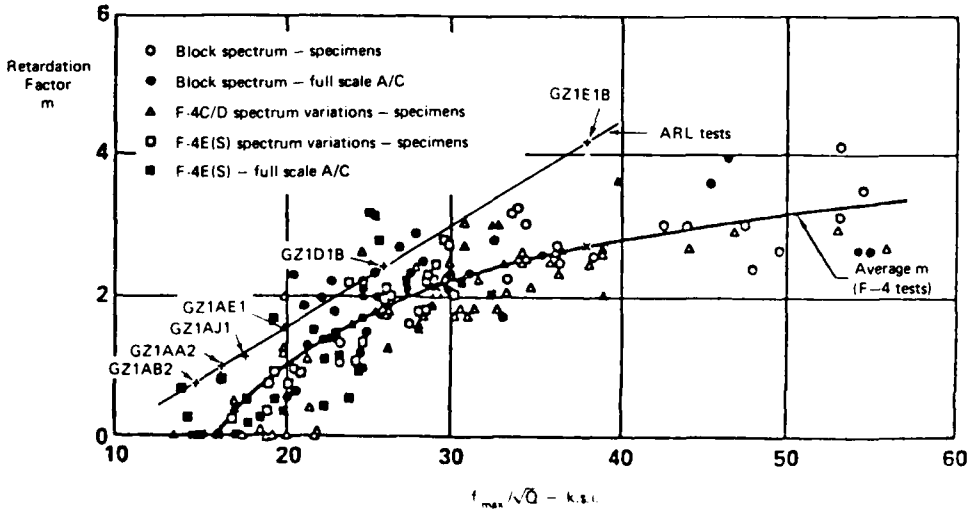

FIG. 9.43 DEPENDENCE OF WHEELER RETARDATION EXPONENT, m, ON MAXIMUM STRESS IN SEQUENCE AND CRACK SHAPE

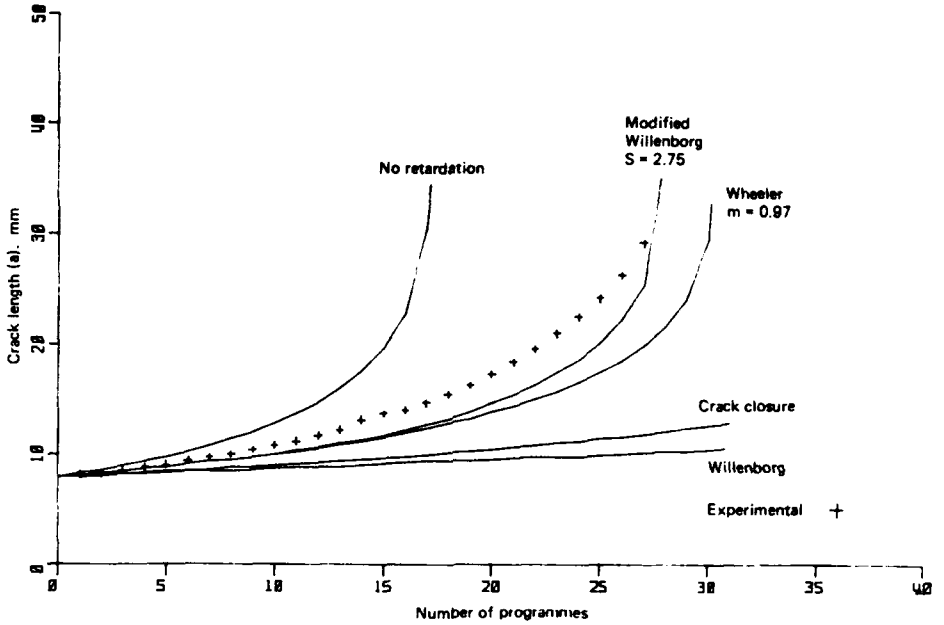

FIG. 9.44 CRACK GROWTH IN 20mm THICK CCT SPECIMEN UNDER THE RAAF 'ALL-TIME-AVERAGE' SEQUENCE (14.12 MPa/g)

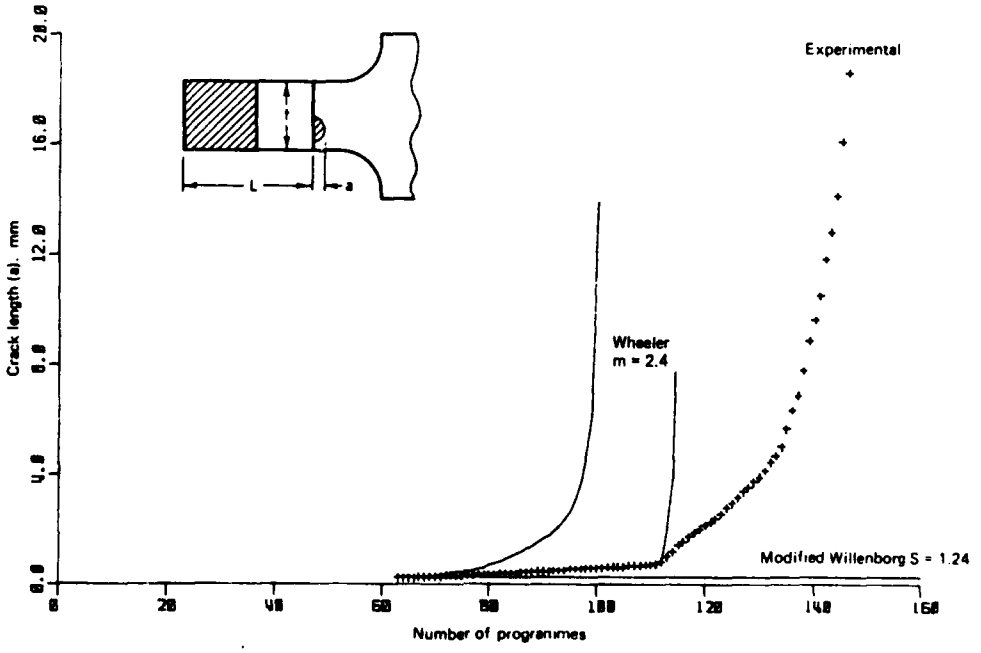

FIG. 9.45 CRACK GROWTH PREDICTION FOR FRAME-BOTTOM SIMULATION SPECIMEN TESTED UNDER THE RAAF 'ALL-TIME-AVERAGE' SEQUENCE (28.63 MPa/g)

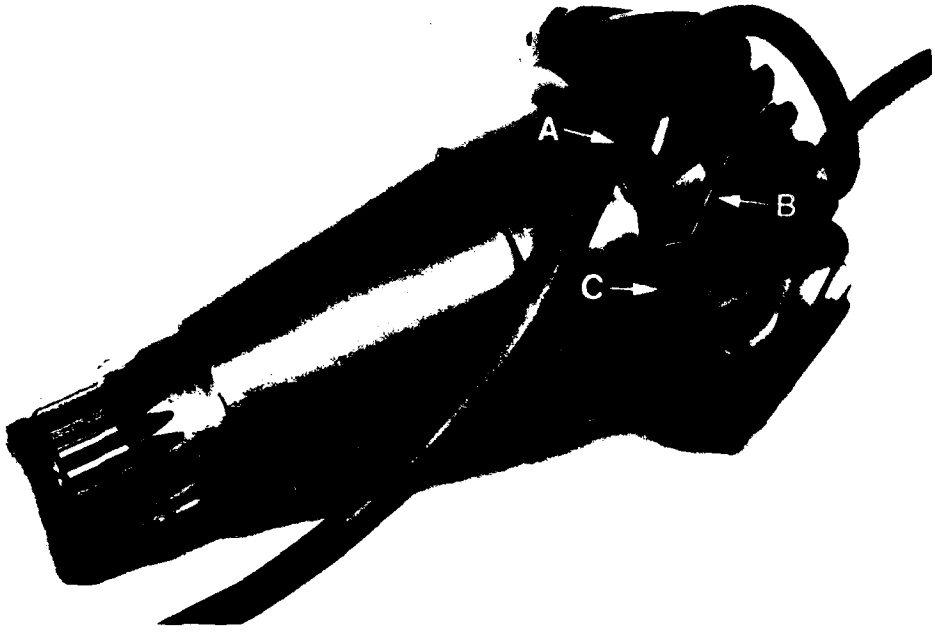

A - Conducting cable position for fluorescent magnetic particle inspection

B - Line of fatigue fracture shown in Fig. 9.47

C - Axial position of separation of pinion

FIG. 9.46 WESTLAND WESSEX POWER INPUT PINION

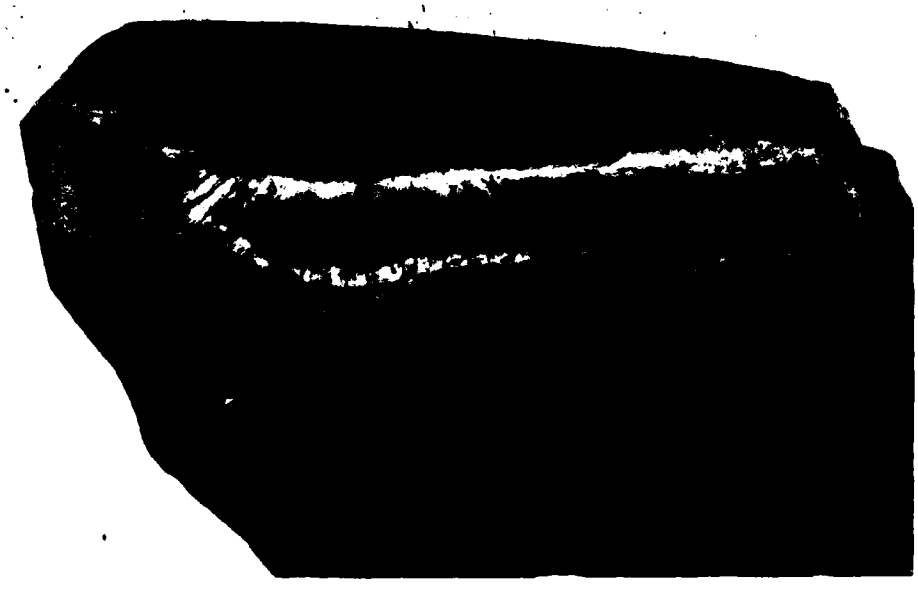

FIG. 9.47 WESTLAND WESSEX POWER INPUT PINION FRACTURE SURFACE

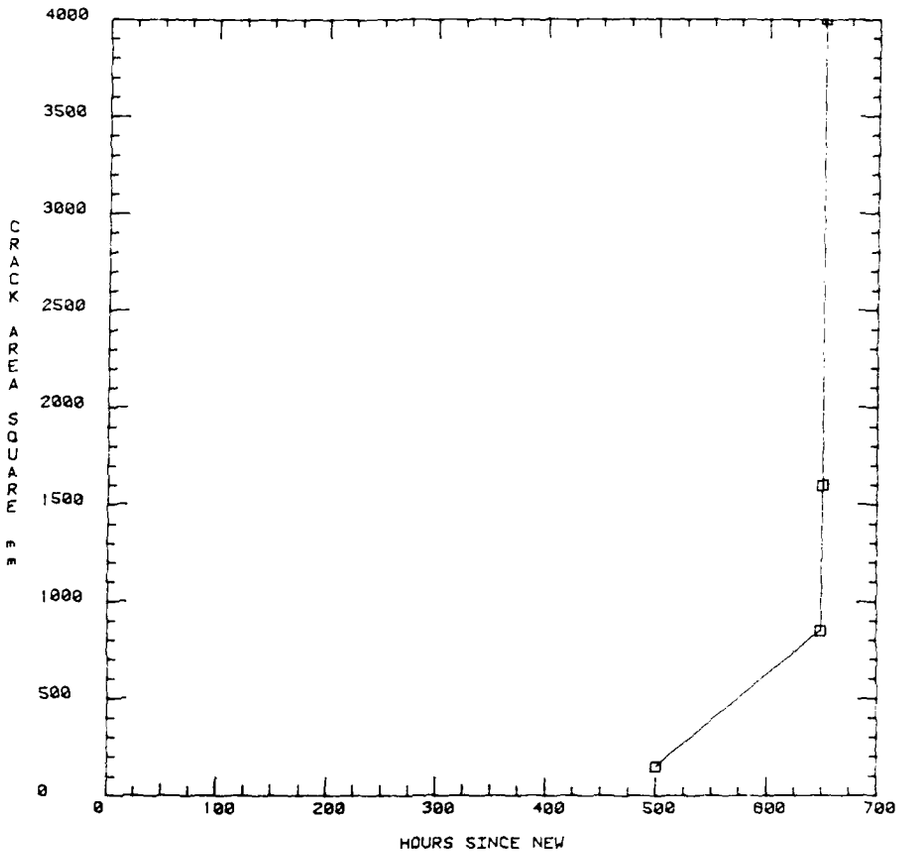

FIG. 9.48 THE PRELIMINARY PLOT OF CUMULATIVE CRACK AREA VS NUMBER OF HOURS SINCE NEW - WESTLAND WESSEX

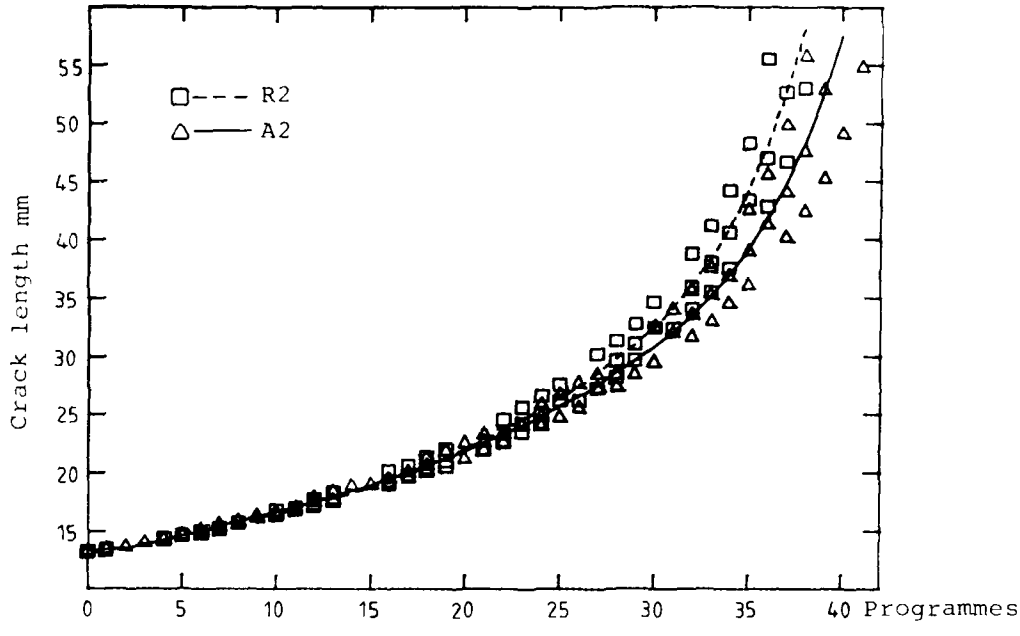

(a) Gross-area stress 11.0MPa/g

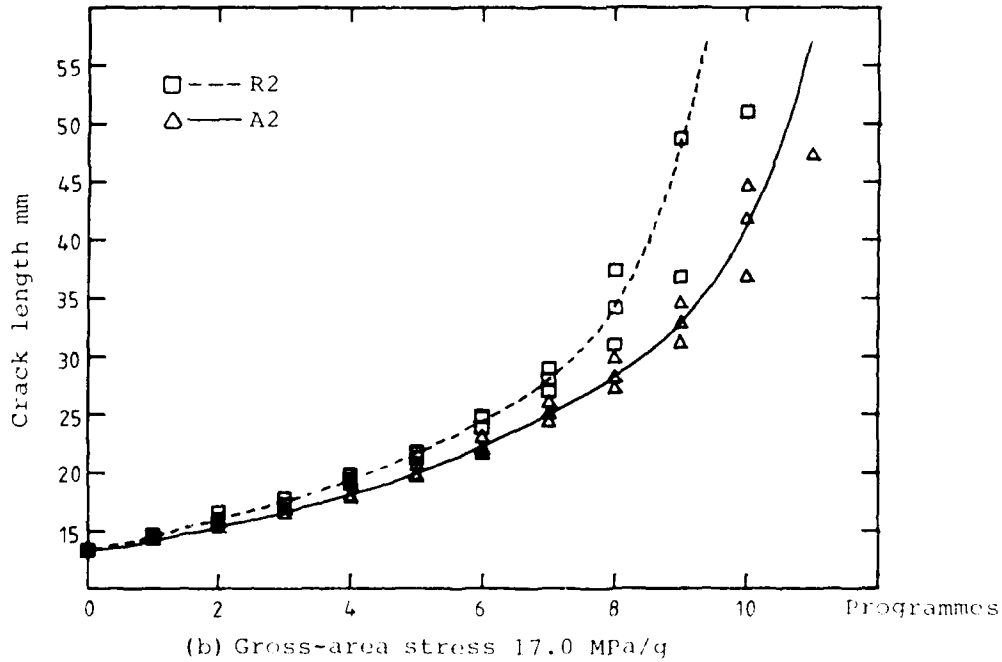

(b) Gross-area stress 17.0 MPa/g

FIG. 9.49 CRACK GROWTH IN CCT SPECIMENS OUTER 'ACCELERATION' SEQUENCE A2, AND 'RETARDATION' SEQUENCE R2

FIG. 9.50 CARBON FIBRE/ALUMINIUM ALLOY BOX BEAM

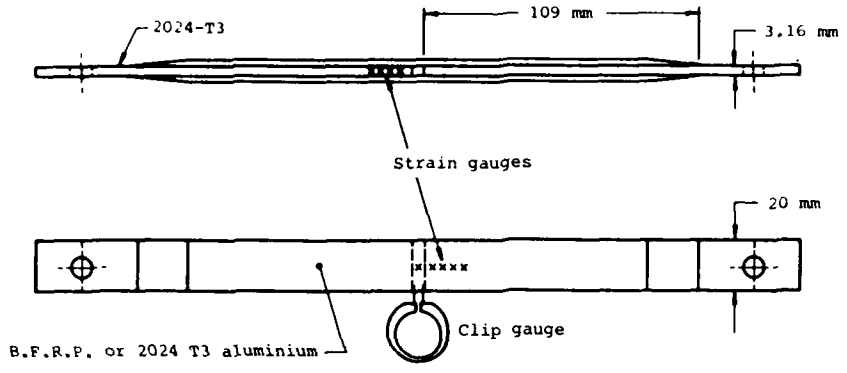

FIG. 9.51(a) ELEMENTAL JOINT SPECIMEN SHOWING POSITION OF CLIP GAUGE USED TO MEASURE DISPLACEMENT Δ

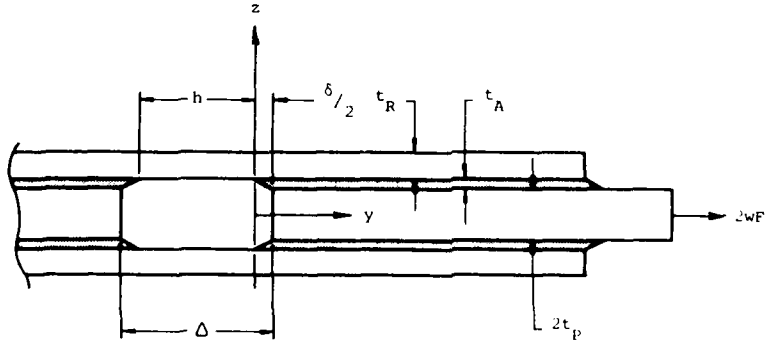

FIG. 9.51(b) NOTATION USED FOR THICKNESSES AND DISPLACEMENTS - ELEMENTAL JOINT SPECIMEN

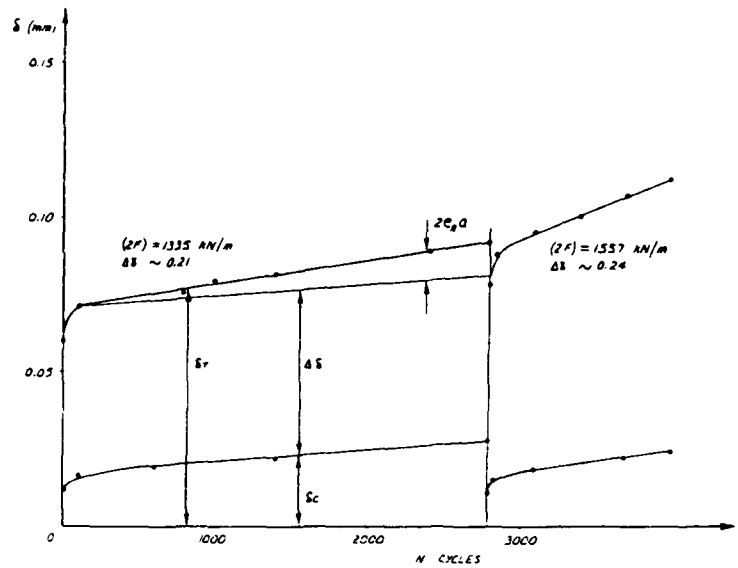

FIG. 9.52 PLOT OF DISPLACEMENT δ FOR TWO LEVELS OF LOAD INTENSITY (2F) VERSUS CYCLES N FOR SPECIMEN WITH BORON/EPOXY OUTER ADHERENDS

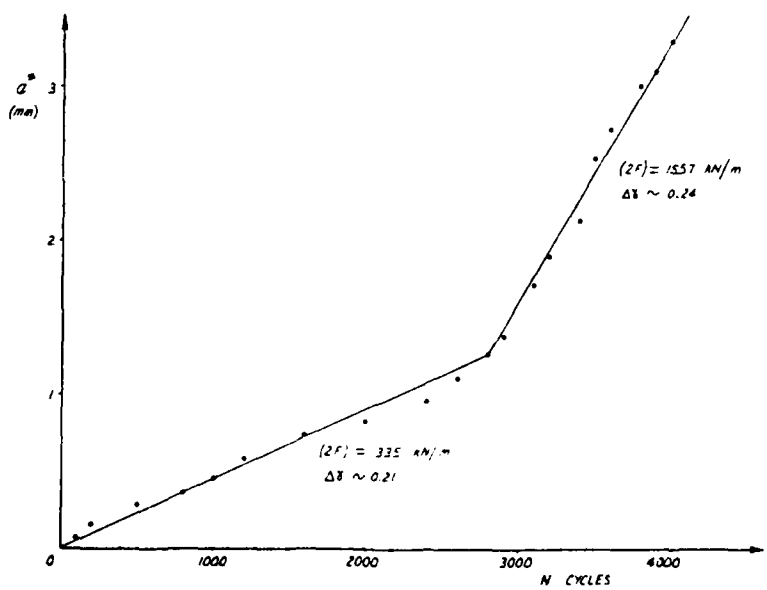

FIG. 9.53 PLOT OF APPARENT CRACK SIZE a* IN THE ADHESIVE LAYERS VERSUS CYCLES N AT TWO LOAD INTENSITY LEVELS, DERIVED FROM FIG. 9.52

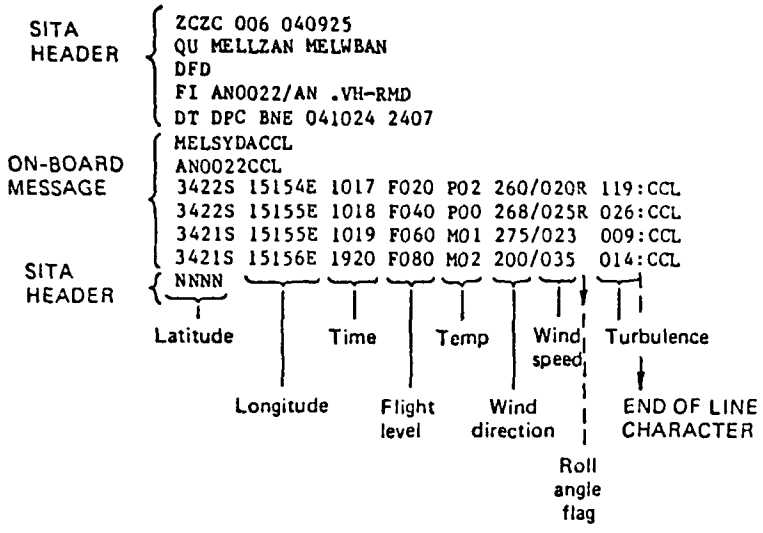

. Latitude and Longitude are in degrees and minutes.

. Time is GMT.

. Temperature is reported with P/M for +/- sign.

. Wind speed is in knots.

. Turbulence is derived equivalent gust velocity in dm/s.

FIG. 9.54 PROPOSED ACARS/AMDAR MESSAGE FORMAT

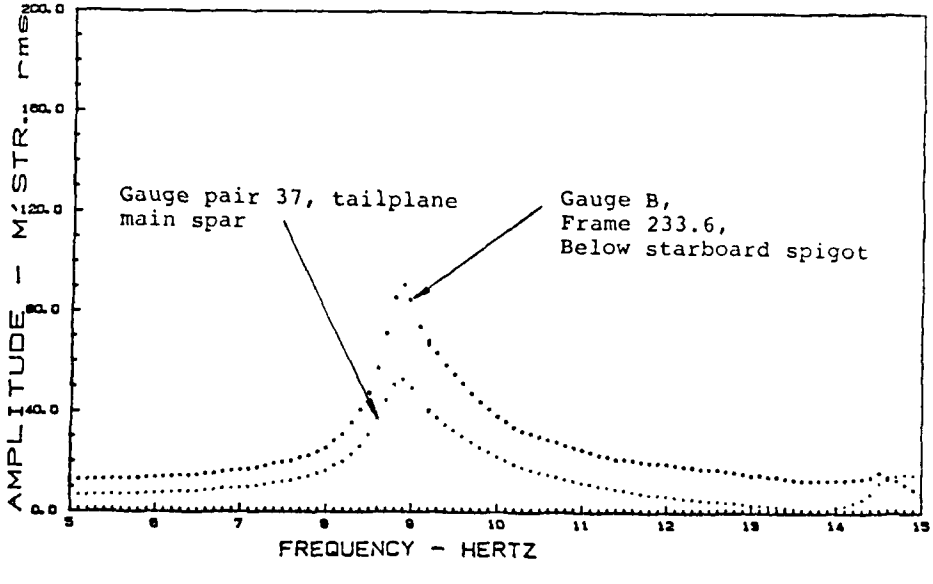

FIG. 9.55 RESONANCE SWEEP OF CT4-A EMPENNAGE

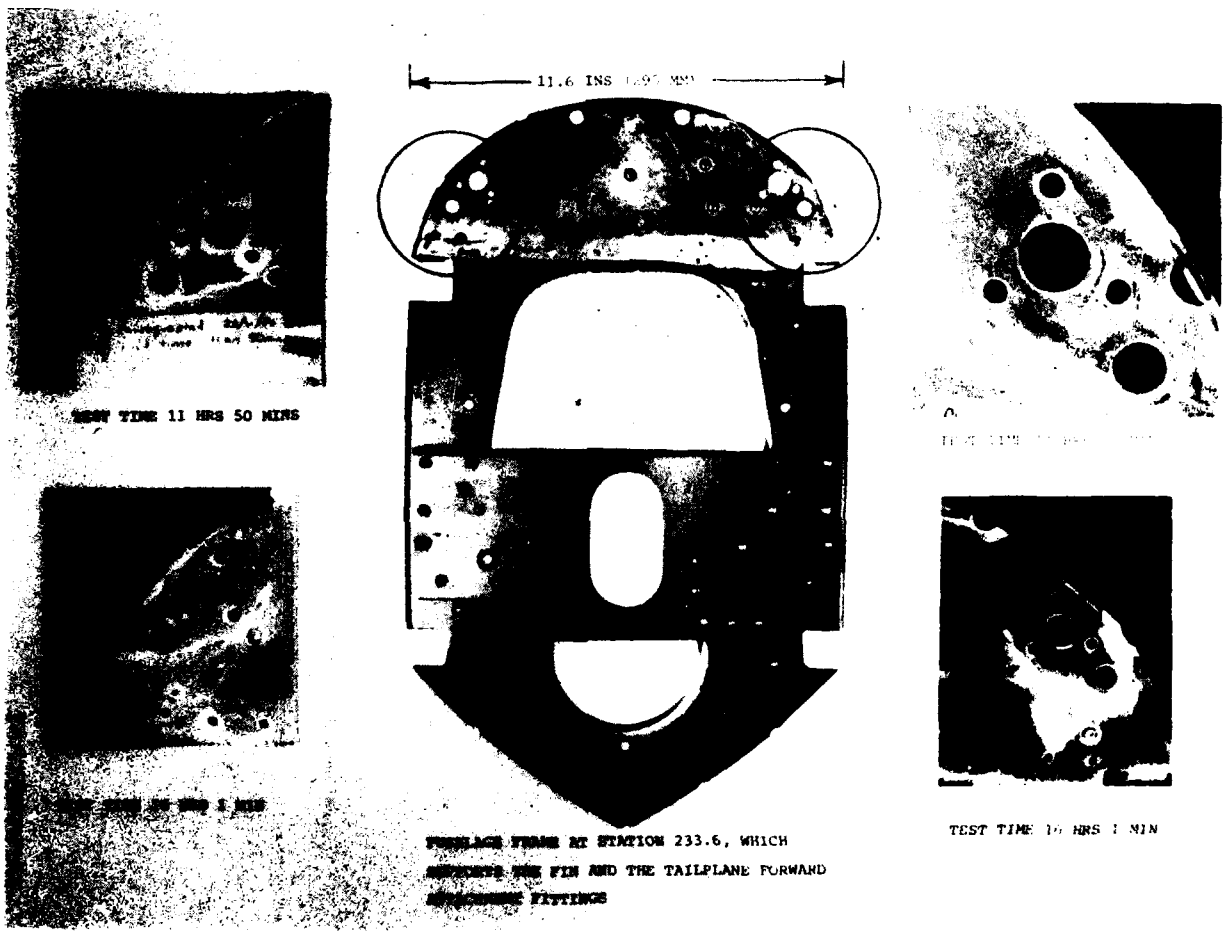

FIG. 9.56 CT4-A EMPENNAGE RESONANCE TEST - FUSELAGE FRAME DAMAGE

DISTRIBUTION

AUSTRALIA

DEPARTMENT OF DEFENCE

DEFENCE CENTRAL

Chief Defence Scientist)
Deputy Chief Defence Scientist)(1 copy)
Superintendent, Science and Program Administration)
Controller, External Relations, Projects & Analytical Studies)
Defence Science Adviser (UK) (Doc Data sheet only)
Counsellor, Defence Science (USA) (Doc Data sheet only)
Defence Central Library
Document Exchange Centre, DISB (18 copies)
Joint Intelligence Organisation
Librarian H Block, Victoria Barracks, Melboaurne
Director General - Army Development (NSO) (4 copies)
Defence Industry and Materiel Policy, FAS

AERONAUTICAL RESEARCH LABORATORIES

Director
Library
Superintendent - Structures
Author: G.S. Jost
J.Y. Mann
B.C. Hoskin
D.G. Ford
C.K. Rider
P.H. Townshend
J.M. Finney
J.G. Sparrow
R. Jones
D.J. Sherman
J.M. Grandage
R.G. Parker
I.A. Anderson
L.R. Gratzer
R.P. Carey
G.S. Jost (for ICAF distribution) (200 copies)
C.K. Rider (for TTCP distribution) (5 copies)
Superintendent - Materials
A.A. Baker
N.E. Ryan
L.M. Bland
B.J. Wicks
I.G. Scott
J.Q. Clayton
N.T. Goldsmith
Superintendent - Aerodynamics
Superintendent - Aeropropulsion
Superintendent - Systems
Principal Engineer

MATERIALS RESEARCH LABORATORIES

Director/Library

DEFENCE RESEARCH CENTRE

Library

RAN RESEARCH LABORATORY
Library

NAVY OFFICE
Navy Scientific Adviser
Directorate of Naval Aircraft Engineering

ARMY OFFICE
Scientific Adviser - Army
Engineering Development Establishment, Library
Royal Military College Library

AIR FORCE OFFICE
Air Force Scientific Adviser
Aircraft Research and Development Unit
Scientific Flight Group
Library
Technical Division Library
Director General Aircraft Engineering - Air Force
HQ Support Command (SLENGO)
RAAF Academy, Point Cook

GOVERNMENT AIRCRAFT FACTORIES
Manager
Library
Mr L.T. Tuller

DEPARTMENT OF AVIATION
Library
Flight Standards Division
Mr C. Torkington
Mr R.B. Douglas

DEPARTMENT OF INDUSTRY, TECHNOLOGY AND COMMERCE
Library

STATUTORY AND STATE AUTHORITIES AND INDUSTRY
Australian Aircraft Consortium Pty Ltd
Manager
Mr G.E. Lawrence
Trans-Australia Airlines, Library
Ansett Airlines of Australia
Library
Mr J.H. Bibo
BHP, Melbourne Research Laboratories
Commonwealth Aircraft Corporation
Library
Mr R.C. Beckett
Hawker de Havilland Aust. Pty Ltd
Library
Mr I.D. McArthur
Qantas Airways Limited, Library

UNIVERSITIES AND COLLEGES

Adelaide	Barr Smith Library
Flinders	Library
La Trobe	Library
Melbourne	Engineering Library
Monash	Hargrave Library
	Professor I.J. Polmear, Materials Engineering
Newcastle	Library

New England	Library
Sydney	Engineering Library
	Dr G.P. Steven
NSW	Physical Sciences Library
	Professor R.A.A. Bryant, Mechanical Engineering
Queensland	Library
Tasmania	Engineering Library
Western Australia	Library

NEW ZEALAND

Defence Scientific Establishment, Library
RNZAF, Vice Consul (Defence Liaison)
Transport Ministry, Airworthiness Branch, Library

UNIVERSITIES

Canterbury	Library
Auckland	Library
Wellington	Library

SPARES (20 copies)

Department of Defence

DOCUMENT CONTROL DATA

1 a AR No	1 b Establishment No	2 Document Date	3 Task No
AR-003-093	ARL-STRUC-TM-399	March, 1985	DEF 82/004

4 Title	5 Security a document	6 No Pages
A REVIEW OF AUSTRALIAN INVESTIGATIONS ON AERONAUTICAL FATIGUE DURING THE PERIOD APRIL 1983 TO MARCH 1985.	UNCLASSIFIED b title c abstract U U	7 No Refs 63

8 Author(s)	9 Downgrading Instructions
G.S. JOST	—

10 Corporate Author and Address	11 Authority (as appropriate) a Sponsor b Security c Downgrading d Approval
Aeronautical Research Laboratories PO Box 4331, MELBOURNE, VIC. 3001	———

12 Secondary Distribution (of this document)

Approved for Public Release.

Overseas enquirers outside stated limitations should be referred through ASDIS, Defence Information Services Branch, Department of Defence, Campbell Park, CANBERRA ACT 2601

13 a This document may be ANNOUNCED in catalogues and awareness services available to ...

No limitations.

13 b Citation for other purposes (ie casual announcement) may be (select unrestricted) or as for 13 a

14 Descriptors	15 COSATI Group
Aircraft	0103
Fatigue (materials)	1113
Structures	
Reviews	
Australia	

16 Abstract

This document was prepared for presentation to the 19th Conference of the International Committee on Aeronautical Fatigue scheduled to be held at Pisa, Italy, on May 20 and 21, 1985. A summary is presented of Australian aircraft fatigue research and associated activities. The major topics discussed include the fatigue of both civil and military aircraft structures, fatigue damage repair and refurbishment and fatigue life monitoring and assessment.

PF 65

This page is to be used to record information which is required by the Establishment for its own use but which will not be added to the DISTIS data base unless specifically requested.

16 Abstract *(Contd)*

17. Imprint

Aeronautical Research Laboratories, Melbourne.

18 Document Series and Number	19. Cost Code	20 Type of Report and Period Covered
Structures Technical Memorandum 399	27 5505	

21. Computer Programs Used

22. Establishment File Ref(s)

END

DATE
FILMED

8 -85

DTIC